CHALMERS

Modeling and Measurements of the Response of Asynchronous Machines Exposed to Voltage Dips

Master of Science Thesis in the Master Degree Programme, Electric Power Engineering

JOHAN ANDERSSON

Department of Energy and Environment
Division of Electric Power Engineering
CHALMERS UNIVERSITY OF TECHNOLOGY
Göteborg, Sweden, 2010

Modeling and Measurements of the Response of Asynchronous Machines Exposed to Voltage Dips

JOHAN ANDERSSON

Department of Energy and Environment
CHALMERS UNIVERSITY OF TECHNOLOGY
Göteborg, Sweden, 2010

Modeling and Measurements of the Response of Asynchronous Machines Exposed to Voltage Dips
JOHAN ANDERSSON

Department of Energy and Environment
Chalmers University of Technology
SE-412 96 Göteborg
Sweden
Telephone + 46 (0)31-722 1000

Chalmers Bibliotek, Reproservice
Göteborg, Sweden 2010

Modeling and Measurements of the Response of Asynchronous Machines Exposed to Voltage Dips

JOHAN ANDERSSON

Depertment of Energy and Enviroment
Chalmers University of Technology

Abstract

Asynchronous machines (induction machines) are widely used in the industry. A high trustiness is required since an interruption of the operation due to a voltage dip can result in both economical losses and safety problems. An example is the security system in a nuclear power plant that includes a high number of asynchronous machines which are driving important pumps and fans. It is therefore of high interest to know how these machines respond to irregular voltages.

This master thesis deals with the dynamical response of asynchronous machines exposed to voltage dips. This is done by simulations in Simulink using the fifth order Park model. To verify the results, simulations of a 4 kW machine has been compared with measurements on a laboratory set-up. Both simulations and measurements are based on disturbance profiles compiled by OKG, the owner of Oskarshamn nuclear power plant.

The results from the simulations agree well with the measurements. It is shown that the speed of the machine is decreased when it is exposed to a decreased voltage. When the voltage recovers the machine draws a higher current from the source due to the magnetization and the acceleration. The magnitude of the current depends on the duration of the dip and on the magnitude of the remaining voltage.

Lightly loaded machines are less affected by voltage dips, under- and over-voltages. This is something that is taken into account by OKG when dimensioning. The aim is to load the machine to a level where the stator current is at rated level when the voltage level is at 85 percent of rated. It means that the machines simulated in this project withstand most of the Disturbance Profiles.

Preface

This report has been written by Johan Andersson as a part of the requirements to obtain a Master of Science degree in Electric Power Engineering. It has been conducted at the division of Electric Power Engineering in collaboration with OKG and Gothia Power AB.

OKG owns and operates three nuclear reactor units, Oskarshamn 1, 2 and 3, which together accounts for ten percent of the total Swedish power generation. OKG is since 1993 an underlying company of E.ON Sweden and has approximately 850 employees.

Gothia Power AB is Swedish consulting company within the electric power field. It is located in Malmö, Gothenburg and Västerås,

Acknowledgement

This master thesis has been carried out at the Department of Energy and Environment, Chalmers University of Technology, in cooperation with OKG and Gothia Power AB.

I would like to thank all those who have helped me conducting this master thesis work.

Daniel Karlsson and Bertil Svensson, Gothia Power, Fredrik Heyman and Jonas Jönsson, OKG, Per Norberg, Chalmers, for providing the project and for support and ideas about the project.

Torbjörn Thirirnger, Chalmers University of Technology, for his support during this master thesis project with precious guidance and many good advices.

Massimo Bongiorno, Chalmers University of Technology, for his help during the measurements in the laboratory set-up.

Eva Palmberg, Chalmers University of Technology, for the help during the compilation of the report.

Johan Andersson
Göteborg, August 2010

List of Symbols

Symbol	Parameter	Unit
$\underline{u}_s$	stator voltage vector	V
u_{qs}	stator voltage in q-direction	V
u_{ds}	stator voltage in d-direction	V
$\underline{i}_s$	stator current vector	A
$\underline{i}_r$	rotor current vector	A
i_{qs}	stator current in q direction	A
i_{ds}	stator current in d-direction	A
i_{qr}	rotor current in q-direction	A
i_{dr}	rotor current in d-direction	A
i_m	magnetizing current	A
i_{qm}	magnetizing current in q-direction	A
i_{dm}	magnetizing current in d-direction	A
R_s	stator resistance	Ω
R_r	rotor resistance	Ω
$L_{s\lambda}$	stator leakage inductance	H
$L_{r\lambda}$	rotor leakage inductance	H
L_s	stator inductance	H
L_r	rotor inductance	H
L_m	magnetizing inductance	H
L_{mq}	magnetizing inductance in q-direction	H
L_{md}	magnetizing inductance in d-direction	H
L_{mdq}	mutual inductance between d- and q-axes	H
L_{qs}	stator inductance in q-direction	H
L_{ds}	stator inductance in d-direction	H
L_{qr}	rotor inductance in q-direction	H
L_{dr}	rotor inductance in d-direction	H
T_e	electrodynamical torque	Nm
T_L	load torque	Nm
J	moment of inertia	kgm^2
ω_r	angular speed of the rotor	rad/s
ω_k	angular velocity of coordinate system	rad/s
ω_s	angular supply frequency	rad/s
p	pole pair number	
Ψ_s	stator flux linkage vector	Wb
Ψ_r	rotor flux linkage vector	Wb
Ψ_m	main flux linkage	Wb
U	voltage column vector	
R	resistance matrix	
I	current column vector	
L	inductance matrix	

List of abbreviations

Abbreviation	Meaning
MSCB	Measurement signal conversion box
MTB	Measurement transducer box
PWM	Pulse Width Modulation
rpm	Revolutions per minute

Table of contents

1 Introduction 1

1.1 Problem background 1

1.2 Related Work 2

1.3 Purpose 2

2 Induction Machine Modeling 3

2.1 Park model 3

2.2 Saturation 4

2.3 Stationary model 6

2.3.1 Machine Torque Calculation 7

2.3.2 Load characteristics 9

2.3.3 Rotational Speed 10

2.4 Table of parameters 11

2.4.1 312 P1 4900 kW 11

2.4.2 327 P1 350 kW 11

2.4.3 712 P2 90 kW 12

3 Network Disturbances 13

3.1 Sources of disturbances 14

3.2 Protection settings 15

4 Case Study 16

4.1 Load rejection 16

4.1.1 Disturbance Profile 2 16

4.2 Shunt faults 17

4.2.1 Disturbance Profile 5 17

4.2.2 Disturbance Profile 7 18

4.3 Wide area disturbances 19

4.3.1 Disturbance Profile 12 19

4.3.2 Disturbance Profile 13 20

5 Experimental Set-up 21

6 Simulations 22
6.1 No saturation considered 22
6.1.1 Disturbance Profile 2 22
6.2 Saturation considered 23
6.2.1 Disturbance Profile 2 23
6.2.2 Disturbance Profile 5 28
6.2.3 Disturbance Profile 7 31
6.2.4 Disturbance Profile 12 35
6.2.5 Disturbance Profile 13 39
6.3 Trip Diagram 41
7 Measurements 43
7.1 The speed-torque curve 43
7.2 Disturbance Profile 2 44
7.3 Disturbance Profile 5 46
7.4 Disturbance Profile 7 49
7.5 Disturbance Profile 12 50
7.6 Disturbance Profile 13 53
8 Conclusion 55
8.1 Future work 57
9 References 59
Appendix A. Determination of the 4 kW asynchronous machine parameters 61

1 Introduction

Asynchronous machines are sensitive to high currents and are usually equipped with load-limiting devices. The protection settings are important, it should trip the machine at high currents to avoid damage due to overheating but it should neither cause unnecessary shutdowns.

1.1 Problem background

The 25th of July 2006, Forsmark 1, which at that time was operated at maximum power output, was subjected to a disturbance. During maintenance work in the 400 kV switchyard, connecting Forsmark unit 1 and 2 to the outer grid, a disconnector was opened due to an incorrect operation instruction. An electrical arc arose over the disconnector and a two phase short circuit occurred which resulted in a drastically decreased voltage at the generator bus bar. At this time unit 2 was shut down due to maintenance. The induced magnetization in unit 1 tried to compensate for the voltage drop. Due to the undervoltage, the 400 kV breakers opened to disconnect the generator from the outer grid, which in turn resulted in an approximately one second voltage peak of about 120 % at the generator bus bar. The voltage transients propagated down through the transformers feeding the local power system and some safety systems (Analysgruppen Bakgrund 2006).

The safety systems include a number of asynchronous machines which are used to drive critical pumps and fans. The machines should, because of safety issues, be able to operate at an input voltage variation of ± 5 %. However, in the procurement of the nuclear power industry the machines are desired to be capable of operating at a voltage level of 85 – 110 % at the motor terminal continuously. The voltage variations can be even worse and therefore it is of great interest to analyze how these machines respond to irregular voltages.

OKG has a policy that the asynchronous machines should not be loaded to more than 85 % in order to fulfill the requirements of withstand voltage levels of 85 – 110 %. The question to be answered in this report is; is that enough?

1.2 Related Work

There has been some research about this subject, how asynchronous machines respond to voltage dips and possible solutions to increase the robustness. For example, Correia de Barros, Leiria, Morched and Nunes (2003) have made a study about how induction motors respond to voltage dips. Their result shows that the response of the motor depends on the time and magnitude of the voltage dip. A similar analysis has been made by Abou-Ghazala, El, Gammal and El-Shennawy (2009). They make the conclusion that most protection settings are too conservative and lead to unnecessary shutdowns.

Owen, Gerardus and Mahadev (1993) have described how the transient stability of an induction machine can be improved by using a fast response voltage regulator, a static VAR compensator (SVC) or a thyristor controlled tap changer (CTC). The idea is to increase the critical time, i.e. the time to decrease the motor speed from rated to critical, which allows longer duration of voltage dips before resulting in disruption of the normal operation.

1.3 Purpose

The purpose of this master thesis report is to analyze the behavior of asynchronous machines when exposed to irregular voltages and frequencies. This will be done by simulations and measurements based on disturbance profiles compiled by OKG, the owner of Oskarshamn Nuclear Power Plant. The aim is to investigate how the machine responds, therefore no protection system is considered in the calculations.

The goal is to study four asynchronous machines. Three of them, 312 P1, 327 P1 and 712 P2 are placed in Oskarshamn unit 2, O2, and the datasheets used in the calculations were given by OKG. Moreover an object is to study a forth machine, a 4 kW machine placed at Chalmers. This is used to verify the simulations by measurements.

Unlike previous research not only voltage dips will be investigated, also under- and overvoltages caused by voltage instability situations and load rejection are studied.

2 Induction Machine Modeling

The fifth-order Park model, sometimes called the two axis model, is used to model the asynchronous machine in Matlab and Simulink in order to analyze the behavior of the machine when exposed to voltage dips.

2.1 Park model

The standard Park model is often based on some simplifying assumptions.

- the field distribution on the air-gap surface is assumed to be a sine wave,
- the effect of saturation is neglected,
- no zero-sequence currents are taken into account.

With these assumptions and all quantities given in a rotating coordinate system with the angular velocity ω_k, the Park model is given by equation (2.1) – (2.4) (Kovács 1984).

$$\underline{u}_s = R_s \underline{i}_s + \frac{d\underline{\Psi}_s}{dt} + j\omega_k \underline{\Psi}_s \tag{2.1}$$

$$0 = R_r \underline{i}_r + \frac{d\underline{\Psi}_r}{dt} + j(\omega_k - \omega_r)\underline{\Psi}_r \tag{2.2}$$

$$\frac{J}{p}\frac{d\omega_r}{dt} = T_e - T_L \tag{2.3}$$

$$T_e = \frac{3}{2} p Im\{\underline{\Psi}_s^* \underline{i}_s\} \tag{2.4}$$

where $\underline{u}_s$, $\underline{i}_s$ and $\underline{\Psi}_s$ are the stator voltage, current and flux vectors, respectively; $\underline{i}_r$ and $\underline{\Psi}_r$ are the rotor current and flux vectors; R_s and R_r are the stator and rotor resistances; J is the moment of inertia of the machine and load; T_e and T_L are the electro dynamical and applied load torque, respectively; p is the number of pole pairs and ω_r the mechanical angular velocity of the rotor. ω_k is the angular velocity of the rotating coordinate system and is in this thesis set equal to the angular supply frequency ω_s.

The stator and rotor flux linkage vectors can according to Thiringer (1996) be expressed as:

$$\underline{\Psi}_s = L_s \underline{i}_s + L_m \underline{i}_r = (L_{s\lambda} + L_m)\underline{i}_s + L_m \underline{i}_r \tag{2.5}$$

$$\underline{\Psi}_r = L_r \underline{i}_r + L_m \underline{i}_s = (L_{r\lambda} + L_m)\underline{i}_r + L_m \underline{i}_s \tag{2.6}$$

where L_s, L_r and L_m are the stator, rotor and magnetizing inductances, respectively; $L_{s\lambda}$ and $L_{r\lambda}$ are the stator and rotor leakage inductances.

If equations (2.5) and (2.6) are inserted in equations (2.1) and (2.2) the asynchronous machine equations can be presented in matrix form:

$$\boldsymbol{U} = \boldsymbol{RI} + \boldsymbol{L}\frac{d\boldsymbol{I}}{dt} \tag{2.7}$$

where **U** is the voltage vector, **R** is the resistance matrix, **I** is the current vector and **L** is the inductance matrix.

$$\boldsymbol{U} = \begin{bmatrix} u_{qs} \\ u_{ds} \\ 0 \\ 0 \\ T_L \end{bmatrix}, \boldsymbol{I} = \begin{bmatrix} i_{qs} \\ i_{ds} \\ i_{qr} \\ i_{dr} \\ \omega_r \end{bmatrix}, \boldsymbol{L} = \begin{bmatrix} L_s & 0 & L_m & 0 & 0 \\ 0 & L_s & 0 & L_m & 0 \\ L_m & 0 & L_r & 0 & 0 \\ 0 & L_m & 0 & L_r & 0 \\ 0 & 0 & 0 & 0 & -\frac{J}{p} \end{bmatrix}$$

$$\boldsymbol{R} = \begin{bmatrix} R_s & L_s\omega_k & 0 & L_m\omega_k & 0 \\ -L_s\omega_k & R_s & -L_m\omega_k & 0 & 0 \\ 0 & L_m(\omega_k - \omega_r) & R_r & L_r(\omega_k - \omega_r) & 0 \\ L_m(\omega_r - \omega_k) & 0 & L_r(\omega_r - \omega_k) & R_r & 0 \\ \frac{3}{2}pL_m i_{dr} & 0 & -\frac{3}{2}pL_m i_{ds} & 0 & 0 \end{bmatrix}$$

u_{qs} and u_{ds} are the quadrature- and direct-axis components of the stator voltage, respectively; i_{qs}, i_{ds}, i_{qr} and i_{dr} are the quadrature- and direct-axis components of the stator and rotor currents, respectively.

2.2 Saturation

Saturation is a non-linear phenomenon that is not taken into account in the Park model described above. In the linear theory the current and flux are proportional and a change in current on the q-axis will not produce any change of flux in the d-axis. But this is not true if saturation is considered, a change in current on the q-axis will cause a change of flux in both axes. To simplify the calculations Hallenius (1982) therefore introduced a mutual inductance L_{mdq} between coils in the d- and q-axis and modified the inductance matrix **L**. The elements in the matrix depend on the currents and has to be determined each time step of the simulation in order to consider the dynamical effects of saturation. The modified L matrix is presented underneath.

$$\boldsymbol{L} = \begin{bmatrix} L_{qs} & L_{mdq} & L_{mq} & L_{mdq} & 0 \\ L_{mdq} & L_{ds} & L_{mdq} & L_{md} & 0 \\ L_{mq} & L_{mdq} & L_{qr} & L_{mdq} & 0 \\ L_{mdq} & L_{md} & L_{mdq} & L_{dr} & 0 \\ 0 & 0 & 0 & 0 & -\frac{J}{p} \end{bmatrix}$$

The matrix elements are derived by Hallenius (1982) but in this report only the equations will be given:

$$L_m = \frac{\Psi_m}{i_m} \tag{2.8}$$

$$i_{dm} = i_{ds} + i_{dr} \tag{2.9}$$

$$i_{qm} = i_{qs} + i_{qr} \tag{2.10}$$

$$i_m = \sqrt{{i_{dm}}^2 + {i_{qm}}^2} \tag{2.11}$$

$$L_{mdq} = \frac{i_{dm} i_{qm}}{i_m} \frac{dL_m}{di_m} \tag{2.12}$$

$$L_{md} = L_m + \frac{{i_{dm}}^2}{i_m} \frac{dL_m}{di_m} \tag{2.13}$$

$$L_{mq} = L_m + \frac{{i_{qm}}^2}{i_m} \frac{dL_m}{di_m} \tag{2.14}$$

$$L_{ds} = L_{s\lambda} + L_{md} \tag{2.15}$$

$$L_{qs} = L_{s\lambda} + L_{mq} \tag{2.16}$$

$$L_{dr} = L_{r\lambda} + L_{md} \tag{2.17}$$

$$L_{qr} = L_{r\lambda} + L_{mq} \tag{2.18}$$

where Ψ_m is the main flux linkage and i_m is the magnetizing current. The mutual inductance L_{mdq} and the variations in L_{md} and L_{mq} are of no consequence in steady state calculations since dL_m/di_m will be zero (Hallenius 1972).

As can be seen, the magnetizing inductance, L_m, is varying with the magnetizing current, i_m. Thiringer (1996) has for a 15 kW asynchronous machine determined L_m as a function of i_m by making a no load test at different levels of voltage. The resulting function was:

$$L_m = 0.05559 - 0.0005679 i_m \tag{2.19}$$

Since the magnetizing inductance as a function of the magnetizing current is not given for all machines, (2.19) has been extrapolated to fit the other machines with the magnetizing inductance at rated speed used as reference. The fact that Thiringer used the power-invariant scaling when determining the magnetizing inductance, while the amplitude-invariant scaling has been used in this project, has also been taken into account.

However, in this study the effect of saturation is mostly of interest in profiles where the voltage level is above the rated one. During voltage dips, when the voltage is low, the

magnetizing current decreases but during swells, when the voltage is high, the same current increases and the magnetizing inductance is turned into saturation.

2.3 Stationary model

Figure 2-1 illustrates the equivalent circuit of the asynchronous machine. The machine is more or less similar to a transformer with two windings, stator and rotor windings, with in this case two air gaps. The stator winding has N_s turns with a total resistance R_s, and the rotor winding has N_r turns with a total resistance R_r. However, by transforming the rotor impedances to the stator side, the circuit can be simplified by removing the transformer. The stator winding produces a flux which for the most part is linked to the rotor winding. The leakage flux, which is proportional to the current, is in the equivalent circuit modeled as an inductance, $L_{s\lambda}$. To create the flux, L_m, which goes from the stator to the rotor it requires a magnetizing current, i_m. Also in the rotor winding there is a leakage flux represented by a leakage inductance, $L_{r\lambda}$ (Hughes 2006).

The behavior of the motor is primarily determined by the slip. If the motor is unloaded the motor will operate close to the synchronous speed with a low slip. If the load torque is increased, the rotor decelerates relative to the traveling flux and the current and power drawn from the supply is increased to provide the mechanical output power. This is represented by replacing the rotor resistance R_r with a fictitious slip-dependent resistance R_r/s (Hughes 2006).

In the iron core there are losses that can be represented by the resistance R_{Fe}, but it is mostly not considered since the term $\omega_s L_m$ has a much smaller value.

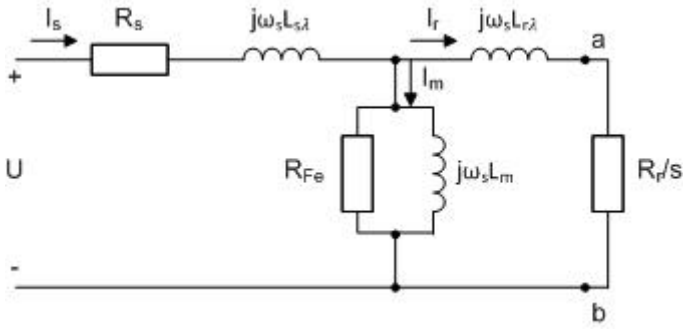

Figure 2-1: Stationary model of an asynchronous machine

2.3.1 Machine Torque Calculation

The stator part, the magnetizing impedance and the rotor leakage inductance can be replaced by a Thevenin equivalent circuit in order to simplify the torque calculations, see Figure 2-2. The motor torque of an asynchronous machine can then be calculated by (2.20) (Hallenius 1972).

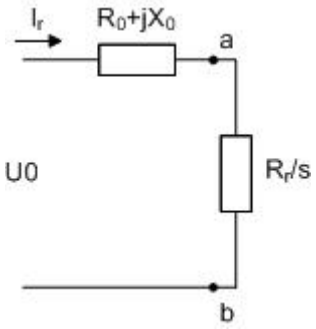

Figure 2-2: Thevenin equivalent circuit of the asynchronous machine.

$$T_m = \frac{P}{\omega_s} = \frac{m}{\omega_s}\frac{R_r}{s}\frac{U_0^2}{\left(R_0 + \frac{R_r}{s}\right)^2 + X_0^2} \tag{2.20}$$

where m is the number of phases and U_0 is the Thevenin equivalent of the stator phase voltage assuming $R_s << X_{s\lambda} + X_m$:

$$U_0 = U\frac{X_m}{X_{s\lambda} + X_m} \tag{2.21}$$

R_0 and X_0 is the real and imaginary part of the Thevenin equivalent inner impedance, Z_0.

$$Z_0 = \frac{X_m(R_s + jX_{s\lambda})}{X_{s\lambda} + X_m} + jX_{r\lambda} = R_0 + jX_0 \tag{2.22}$$

In Figure 2-3 - 2-6 the calculated motor torque curves of the machines that are investigated in this report are presented. As can be seen there are some differences between the curves. For example, the 4900 kW machine in Figure 2-6 has a steeper torque curve in the normal operation region compared to the other which is due to a smaller rotor resistance.

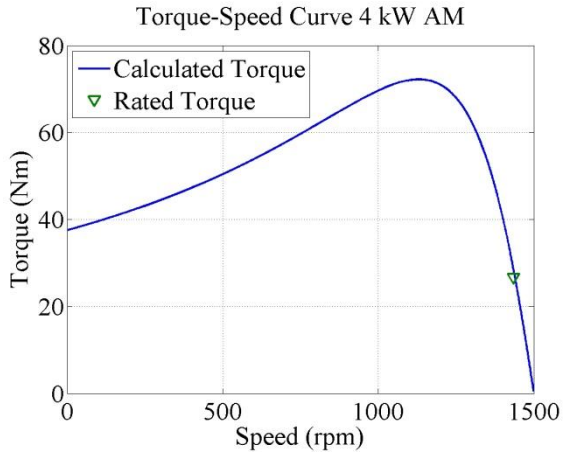

Figure 2-3: Motor torque as a function of speed of the 4 kW asynchronous machine.

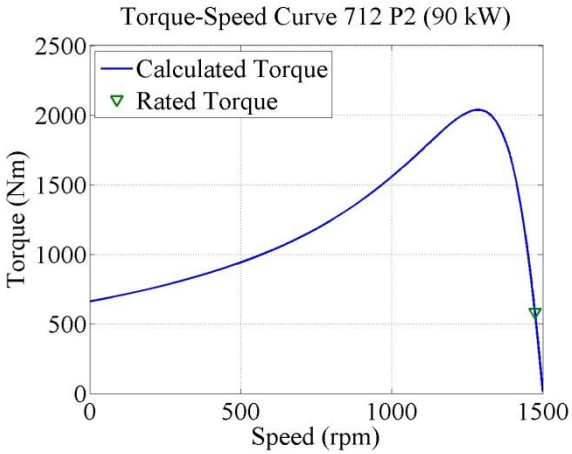

Figure 2-4: Motor torque as a function of speed of the 90 kW asynchronous machine.

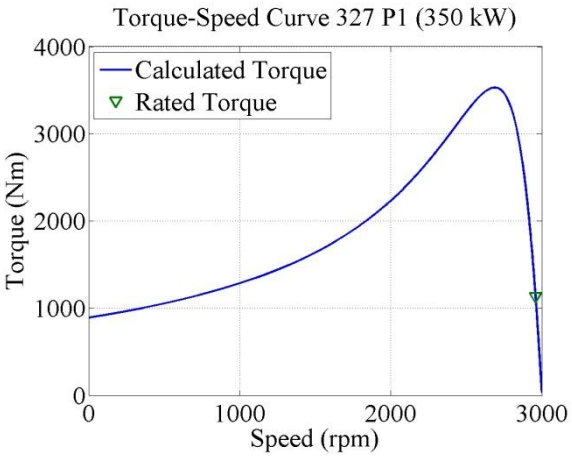

Figure 2-5: Motor torque as a function of speed of the 350 kW asynchronous machine.

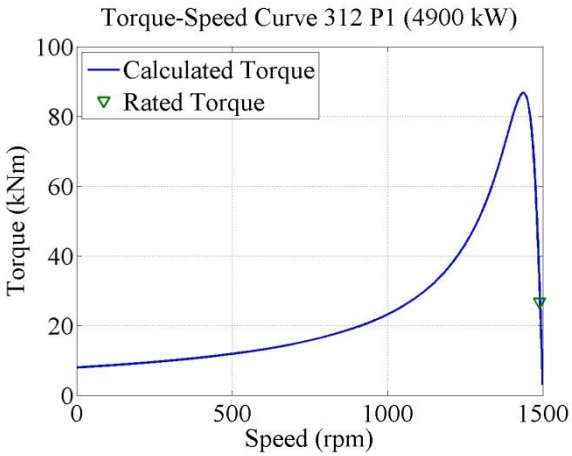

Figure 2-6: Motor torque as a function of speed of the 4900 kW asynchronous machine.

2.3.2 Load characteristics

The asynchronous machines are loaded with pumps and the load torque characteristics of these can be expressed as:

$$T_L = kn^2 \tag{2.23}$$

where k is a constant and n is the mechanical speed.

OKG aims to not run the asynchronous machines at rated load in order to increase the safety margins at variations in the voltage level. In this project the load torque is chosen in such a way that the current reaches rated level at a voltage level of 85 percent.

This constant k is chosen in such a way that the load torque (2.23) is equal to the motor torque (2.20) when the asynchronous machine is loaded according to previous statement.

Table 2-1: The value of constant k in equation 2.23.

Asynchronous machine	k
712 P2 (90kW)	0.000228
327 P1 (350kW)	0.000107
312 P1 (4900kW)	0.011500

2.3.3 Rotational Speed

The rotational speed of an asynchronous machine is decided by the relation between the mechanical load torque and the torque-speed characteristics of the machine. The operation point is at the speed where the load torque is equal to the machine torque, $T_m=T_l$. However, this relation is not enough to determine if it is a stable operating point or not (Hallenius 1972).

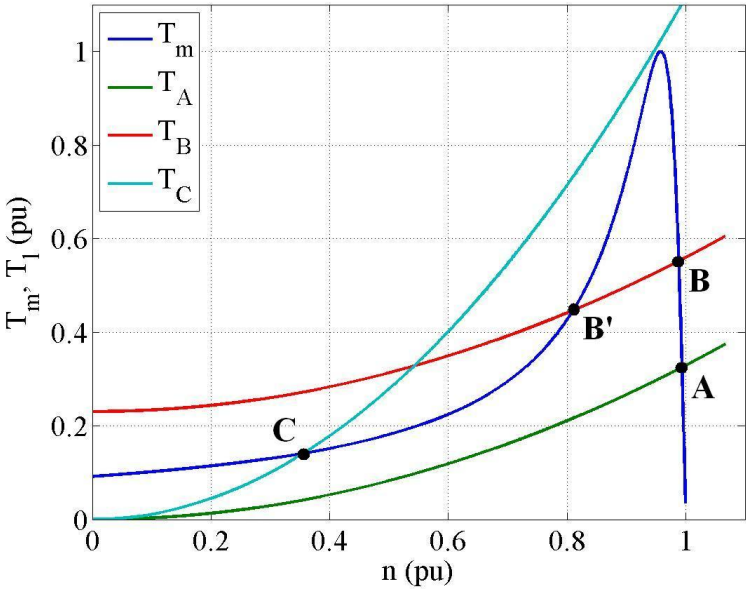

2-7: The torque-speed characteristics of an asynchronous machine, T_m, together with three different load torque characteristics, T_A, T_B and T_C.

The criterion of a stable operation is that the derivative of the load torque characteristics is higher than that of the machine in the operation point (Hallenius 1972):

$$\left(\frac{dT_l}{dn}\right) > \left(\frac{dT_m}{dn}\right)_{T_l=T_m} \tag{2.24}$$

It is clear that point A and B are satisfying the criterion in (2.24). Point B' is satisfying $T_{B'}=T_m$ but not the criterion in (2.24) and is for that reason not stable. If the machine is forced by increasing the load to operate in point B', there are two scenarios that can occur.

- A disturbance in rotational speed in negative direction results in an increase of braking torque and the machine will stop.
- A disturbance in rotational speed in positive direction results in an increase of torque in positive direction and the machine will accelerate until it reaches the stable operating point in B.

In point C both criteria are satisfied but the machine would be highly overloaded and overheated (Hallenius 1972).

2.4 Table of parameters

In this Section the parameter values, given from OKG, of the investigated machines can be found. For the 4 kW machine the parameters are measured and presented in Appendix A.

The measured resistances and reactances are presented in per units and to transfer into physical quantities the rated power and voltage are used as bases. From them the impedance base is calculated:

$$Z_{base} = \frac{V_{base}^2}{S_{base}} \tag{2.25}$$

2.4.1 312 P1 4900 kW

Table 2-2: Table of parameters of the 312 P1 4900 kW machine.

Parameter	Symbol	Data value	Computed value	Unit
Rated power	S_n	5.532		MVA
Rated voltage	V_n	6.3		kV
Rated current	I_n	507		A
Starting current	I_{st}	2864		A
Rated speed	n_n	1490		rpm
Slip	s	0.007		
Inertia	J	350		kgm^2
Rated torque	T_n	31420		Nm
Stator resistance	R_s		0.0183	pu
Rotor resistance at rated operating	R_r		0.0072	pu
Rotor resistance at start	R_{rst}		0.0169	pu
Stator leakage reactance	$X_{s\lambda}$		0.0867	pu
Rotor leakage reactance	$X_{r\lambda}$		0.0867	pu
Magnetizing resistance	R_m		0.1182	pu
Magnetizing reactance	X_m		2.363	pu

2.4.2 327 P1 350 kW

Table 2-3: Table of parameters of the 327 P1 350 kW machine.

Parameter	Symbol	Data value	Computed value	Unit
Rated power	S_n	0.404		MVA
Rated voltage	V_n	6.3		kV
Rated current	I_n	37		A
Starting current	I_{st}	259		A
Rated speed	n_n	2960		rpm
Slip	s	0.013		
Inertia	J	10.7		kgm^2
Rated torque	T_n	1130		Nm
Stator resistance	R_s		0.0414	pu
Rotor resistance at rated operating	R_r		0.0138	pu
Rotor resistance at start	R_{rst}		0.0222	pu
Stator leakage reactance	$X_{s\lambda}$		0.0640	pu
Rotor leakage reactance	$X_{r\lambda}$		0.0640	pu
Magnetizing resistance	R_m		0.1218	pu
Magnetizing reactance	X_m		2.4369	pu

2.4.3 712 P2 90 kW

Table 2-4: Table of parameters of the 712 P2 90 kW machine.

Parameter	Symbol	Data value	Computed value	Unit
Rated power	S_n	0.111		MVA
Rated voltage	V_n	0.38		kV
Rated current	I_n	168		A
Starting current	I_{st}	1160		A
Rated speed	n_n	1475		rpm
Slip	s	0.017		
Inertia	J	2		kgm^2
Rated torque	T_n	580		Nm
Stator resistance	R_s		0.0322	pu
Rotor resistance at rated operating	R_r		0.0187	pu
Rotor resistance at start	R_{rst}		0.0329	pu
Stator leakage reactance	$X_{s\lambda}$		0.0647	pu
Rotor leakage reactance	$X_{r\lambda}$		0.0647	pu
Magnetizing resistance	R_m		0.0943	pu
Magnetizing reactance	X_m		1.8862	pu

3 Network Disturbances

Network disturbances may be caused by various events in the power system. What characterizes them is a variation in voltage and/or frequency. It could be a temporary decreased voltage level, voltage dip, or temporary increased voltage level, swell. In the worst case a total voltage collapse could occur.

IEEE defines voltage sags as a variation of the rms value of the voltage or current from the nominal during a period of 0.01 seconds to 1 minute. The typical voltage magnitude during these sags is 0.1 to 0.9 pu (IEEE). IEC is using the term voltage dip to describe this phenomenon, but both terms are considered to be interchangeable (Beaty, Dugan & McGranaghan 1996). In this report voltage dip will be used to describe a temporary decrease in voltage.

A voltage dip is often presented in percent and it can be confusing whether a for example 30 percent voltage dip corresponds to a voltage level of 0.7 pu or 0.3 pu. In this report it represents the remaining voltage, in this case 0.3 pu. This is illustrated in Figure 3.1.

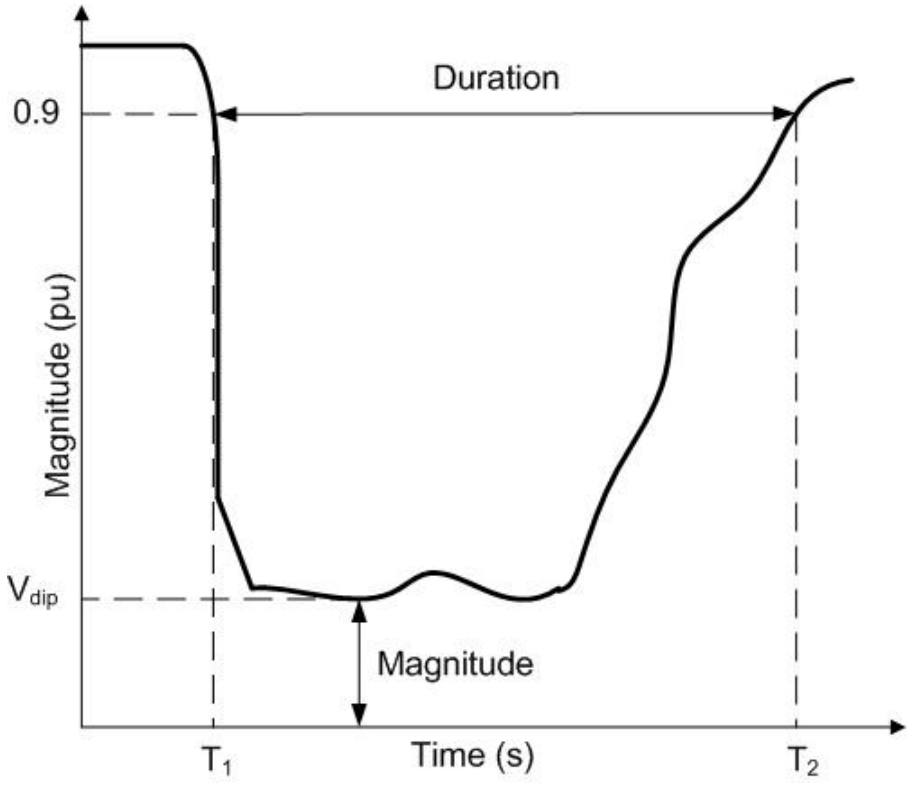

Figure 3-1: An illustration of the definition of a voltage dip.

A drop in terminal voltage will lead to a reduction in torque and the motor will decelerate until it reaches a new operating point. If the terminal voltage dip is too large the load torque will be higher than the pull-out torque and the motor will continue to decelerate (Bollen 2000).

In Figure 3-2 the speed torque curves of the 4900 kW machine are presented, both during normal operation and during a 60 percent voltage dip, together with the load torque of a pump. As mentioned in Section 2.3.3 the operating point of the machine is the point where the load torque is equal to the motor torque, in this case at a speed of 1491 rpm. When the motor is exposed to the 60 percent voltage dip it will decelerate until it reaches a new operating point where the motor and load torque are in equilibrium. In this case the load torque will not be higher than the pull-out torque and the motor will find the new operating point at 1463 rpm. However, if the machine is operating in this point for a too long time there will be a high risk of damage the machine due to overheating. If the voltage dip would have been slightly lower, the motor would continue to decelerate into unstable operation. When the voltage is recovered, the motor will accelerate until a new equilibrium is reached.

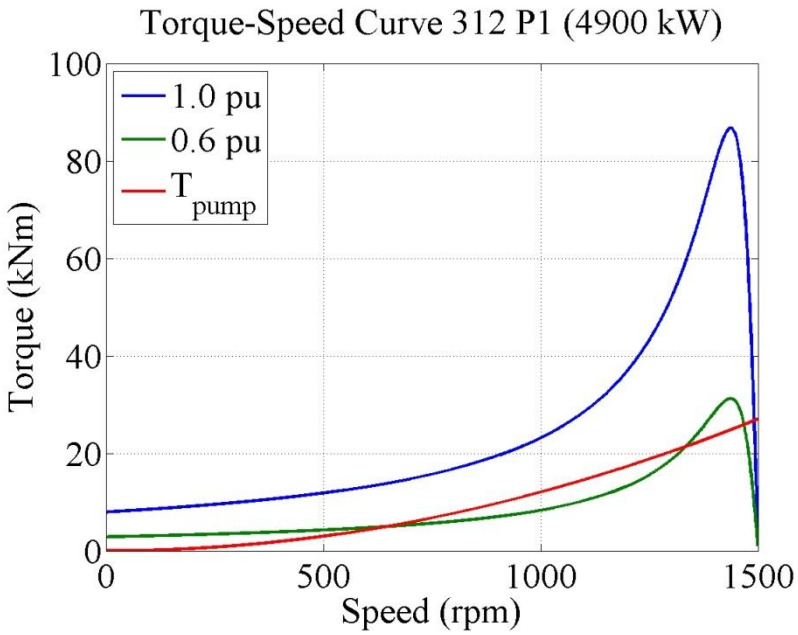

Figure 3-2: The motor torque characteristics of the 4900 kW asynchronous machine during normal operation and during a 60 percent voltage dip together with the load torque of the pump.

There are a number of phenomena that can make the motor stall due to a voltage dip. First of all, deep dips will cause high torque oscillations when the dip occurs and when the voltage recovers. This can damage the motor or lead to process interruptions. Secondly, when the voltage recovers the field in the airgap has to be built up again. This can take up to 100 ms and during this time the motor continues to decelerate. Another phenomenon is the high inrush current when the voltage recovers, first to build up the airgap field and then to accelerate the motor (Bollen 2000).

3.1 Sources of disturbances

Voltage dips can occur due to a variety of reasons, e.g. lightning strikes at or close to transmission lines, equipment failure, start of electrical machines and incorrect treatment. Other disturbances can be load rejection that results in overvoltage or lack of power transmission capacity resulting in a voltage instability.

3.2 Protection settings

In the industry, electrical machines are equipped with protection systems to prevent damage by tripping them at e.g. phase overcurrent, low voltage or locked rotor, caused by voltage dips.

In the datasheet of the motor protection relay MotorMaster 200 from Alstom, a thermal curve is presented, see Figure 3-3. This curve indicates how long time the machine can be exposed to a multiple of the rated current before the motor protection relay trips the machine, the machines will probably withstand a little bit higher current. However, this curve will be used to compare the robustness of the machines when loaded to different degrees.

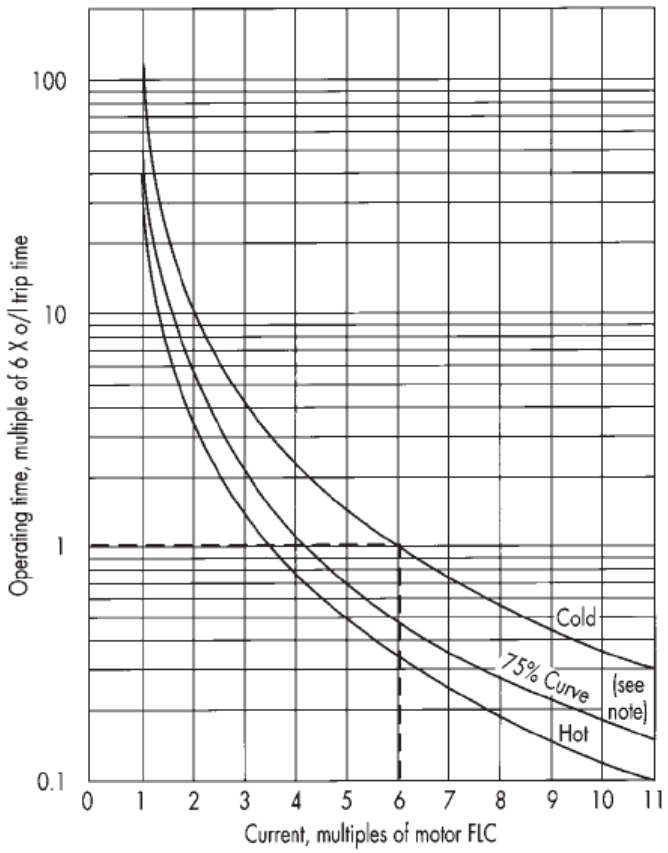

3-3: Thermal curve (Alstom).

4 Case Study

Since 2000 a number of power system studies of Oskarshamn's three units have been performed. The generator voltage level during three phase faults, phase to phase short circuits and single phase to ground faults has been studied, both with correct operation and with failure in operation of the protection systems. By statistics and experiences from these studies a couple of events have been selected for simulations. From the simulations, 13 disturbance profiles have been developed. Of course, in reality the power plant experiences several more transient profiles, but the profiles are chosen so that the most extreme and difficult situations are covered (NEA 2009).

The disturbance profiles consist of voltage and frequency profiles, but in the cases where the frequency is almost constant it is not presented. Out of the 13 disturbance profiles, five have been chosen, in collaboration with OKG, to be further analyzed in this report. The rest of them are considered to be covered by the chosen ones.

4.1 Load rejection

Load rejection occurs if the power plant is disconnected from the transmission system by the breaker. This may be caused by inadvertent operation of the breaker due to failure in the operating mechanism or by incorrect trip signals from the control system (NEA 2009).

4.1.1 Disturbance Profile 2

Disturbance Profile 2, Figure 4-1, may be caused by a load rejection due to e.g. an inadvertent operation of the breaker at the high voltage side of the step-up transformer during operation with full production in field current regulator control mode. Switching frome automatic voltage control to FCR can be caused by faults in two regulator channels at the same time. (NEA 2009).

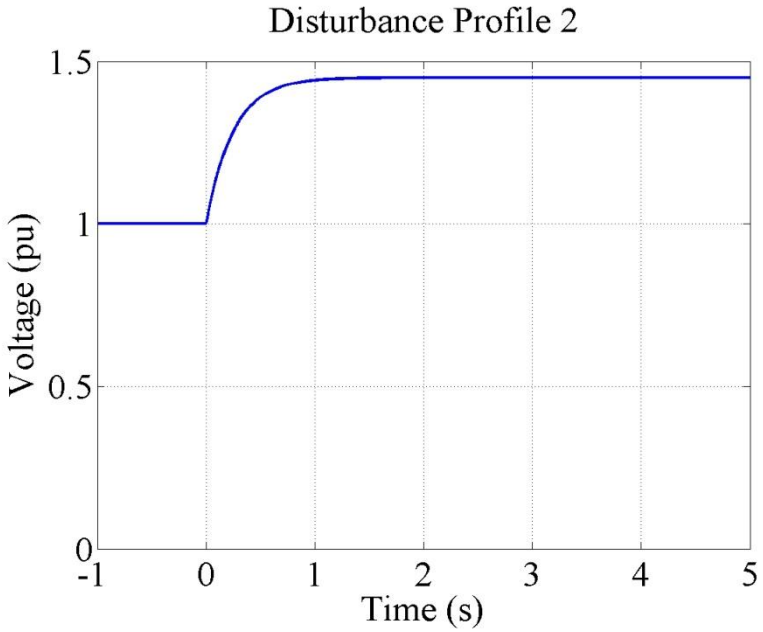

Figure 4-1: Voltage profile 2 representing a load rejection in FCR control mode.

4.2 Shunt faults

A shunt fault is a short circuit between phases or one phase and the ground. In the transmission system they are mainly caused by lightning strokes at or close to the transmission line (NEA 2009).

4.2.1 Disturbance Profile 5

Disturbance Profile 5 represents the requirements of power production for large and medium-sized nuclear power stations from Svenska Kraftnät. The voltage dip can be caused by close-up three-phase faults on an outgoing transmission line when the line circuit breaker fails to interrupt the fault current. The Breaker Failure Protection reacts and trips the adjacent circuit breakers which clear the fault. When this is done, the voltage slowly recovers due to a voltage drop across the transient reactance of the generator (NEA 2009).

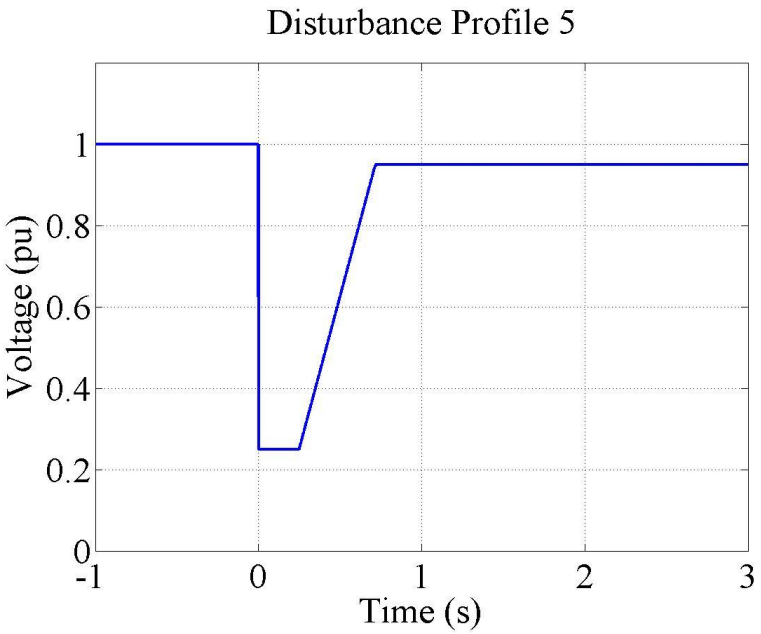

Figure 4-2: Voltage Profile 5 (The NORDEL Voltage) representing a close-up three-phase fault on an outgoing transmission line when the line circuit breaker fails to interrupt the fault current.

4.2.2 Disturbance Profile 7

Disturbance Profile 7 is representing the incident described in the introduction. The voltage dip is caused by a three-phase fault on the busbar connecting the power plant with the transmission system. The busbar protection is considered to fail and the underimpedance protection, which is the backup protection for this kind of failure, generates a trip signal for the breaker of the high voltage side of the generator step-up transformer. After the fault is cleared the power plant is disconnected from the grid to operate in house load operation (NEA 2009).

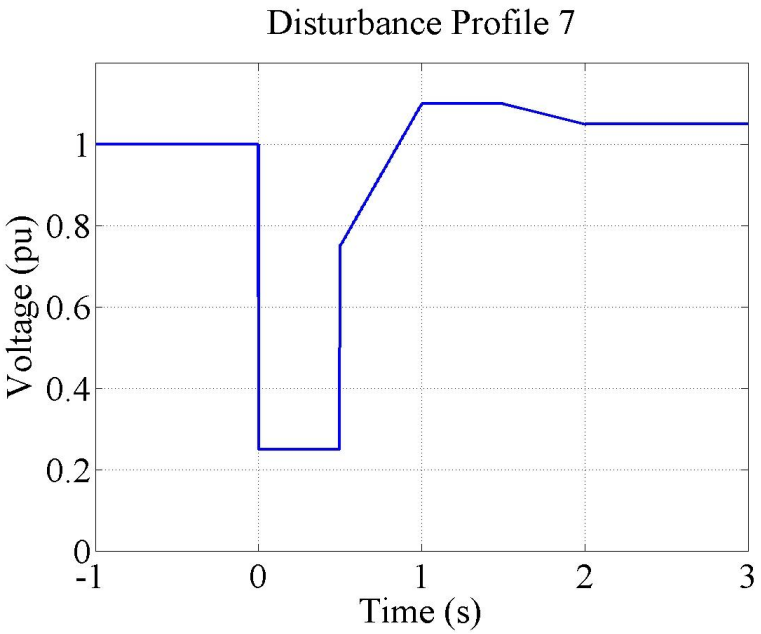

Figure 4-3: Voltage Profile 7 representing a three-phase fault of the busbar connecting the power plant to the grid when the busbar protection system fails to operate.

4.3 Wide area disturbances

Wide area disturbances affect the entire or a large part of the power system. This kind of disturbance is exceptional and is generally caused by a decreasing capability to produce and/or transfer enough power (NEA 2009).

4.3.1 Disturbance Profile 12

Disturbance Profile 12 is representing a voltage collapse like in Sweden 1983 and Koeberg, South Africa, 1998. It is not possible to predict the course of events of the disturbance since it originates from a lot of different events and failures.

The voltage and frequency Profiles in Figure 4-4 and 4-5 are developed on the basis that the power plant is connected to a part of the power system with a lack of generation and where the voltage collapses after around ten minutes. The voltage drop is usually caused by losses of a number of transmission lines or losses of production, often in combination with losses of transmission lines.

During the first ten minutes the voltage is decreasing with three percent per minute until the voltage level is at 70 percent of the nominal. Then the reduction in voltage is increased to 20 percent per second. The grid frequency will remain stable the first ten minutes after the voltage collapse is initiated and then it decreases with 5 Hz per second.

If the power transfer is higher, the voltage will probably decrease faster (NEA 2009).

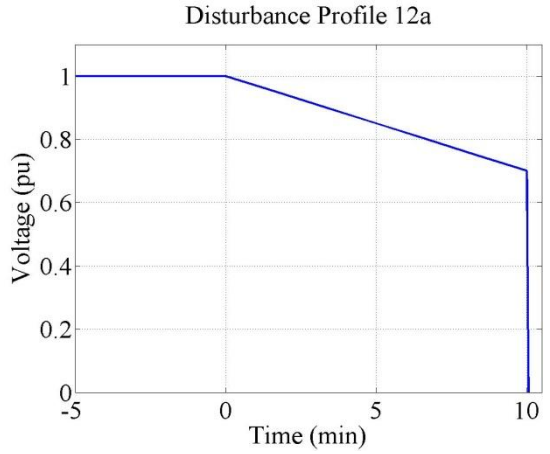

Figure 4-4: Voltgage Profile 12 representing the voltage collapse in Koeberg, South Afrika, 1998.

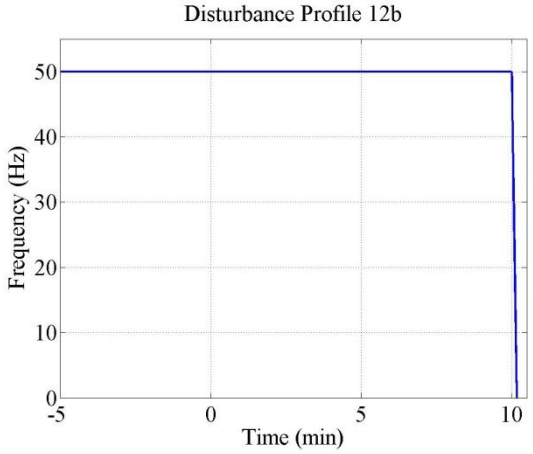

Figure 4-5: Frequency Profile 12.

4.3.2 Disturbance Profile 13

Disturbance Profile 13 represents voltage and frequency variations in the transmission system when manual load shedding is used to prevent a voltage collapse. In the south of Sweden gas turbines can be used to control the voltage level at disturbances, but these cannot be synchronized to the grid at lower voltages than 90 percent of the nominal grid voltage. If a load shedding system is installed the voltage level can be stabilized at a lower level, but if it decreases beneath 70 percent a system breakdown will most likely occur. Therefore the voltage dip is expected to be stabilized at 80 percent in the voltage profile which has been compiled from recordings of disturbances in Finland and South Africa. The rate of change in voltage level is set to five percent per minute.

When load shedding is applied there will be a surplus of generation in the power system which may lead to an increase in frequency. For a large thermal power plant the upper frequency threshold to comply with is set to 51 Hz, specified by Svenska Kraftnät. Therefore the frequency profile is designed with a stabilization level of 51 Hz and a rate of change of frequency of 0.33 Hz per minute (NEA 2009).

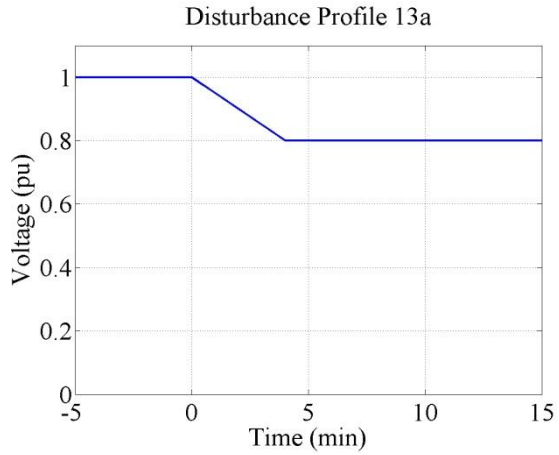

4-6: The voltage variation during Disturbance Profile 13.

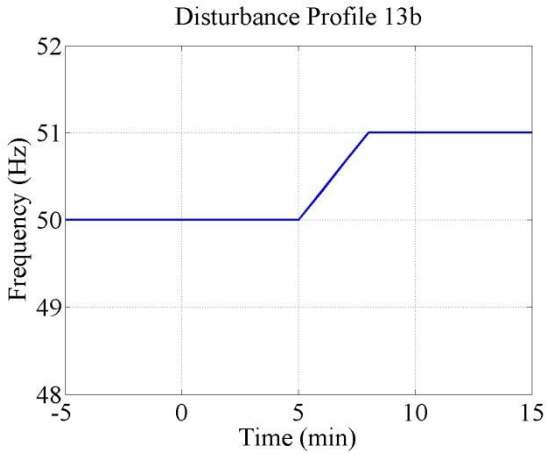

4-7: Frequency Profile 13.

5 Experimental Set-up

To verify that the results from the simulations are reasonable, experiments have been performed on a 4 kW asynchronous machine. It is fed via a DC to AC inverter connected to a 400 V DC source.

Between the inverter and the asynchronous machine a measurement transducer box, MTB, is connected in order to measure the actual stator voltage and current of the machine. The measured signals are then sent to a measurement signal conversion box, MSCB, which also receives measurement signals of the DC voltage and current directly from the inverter. The current signals are converted into voltages and then all signals are sent to the computer control system via a D-Space interface.

The computer contains an open loop controller created in Simulink and D-Space by Dr. Massimo Bongiorno, Chalmers. In the controller a reference signal of a chosen voltage dip is created and compared to a PWM-signal and the duty cycles for the switches in the inverter are given. The inverter is assumed to be an infinitely large bus able to deliver the power that the machine demands. Therefore no feedback is needed in the controller.

The on/off signals are transmitted to an Opto sending and receiving conversion card, OSRCC, via the D-Space interface and further to the switches in the inverter. The switches are then switching according to the duty cycles calculated in the controller in order to generate a voltage dip corresponding to the reference signal.

To not damage the machine, fuses of 10 and 16 ampere are used depending on whether the machine is delta or why connected.

The asynchronous machine is loaded with a DC-machine that is connected to the shaft and operating in generation mode. It takes mechanical power from the asynchronous machine and feds it back to the electrical grid. In that way the load torque is easy to change by changing the armature current of the DC-machine.

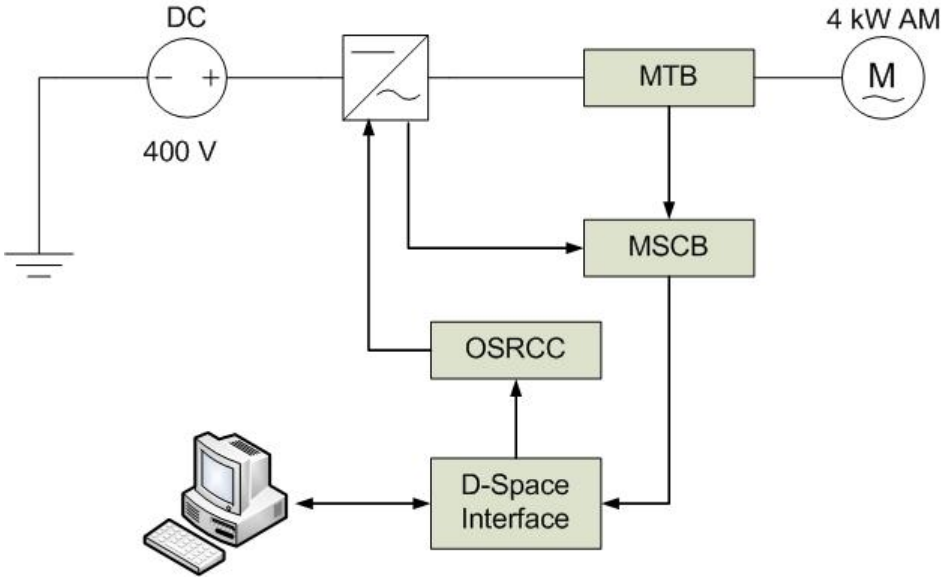

5-1: The experimental set-up.

6 Simulations

In this chapter, the results from the simulations of the asynchronous machine model are presented. As mentioned earlier the Park model is not considering any saturation effects of the magnetizing inductance, however these effects are implemented by using the L matrix presented in Section 2.2. To see how this implementation is affecting the machine, simulations has been performed both when saturation is considered and not. The machines is mainly affected by saturation at higher voltage levels, therefore this comparison has only been performed for Disturbance Profile 2.

6.1 No saturation considered

In this section simulation of the 4900 kW machine has been performed without considering any saturation.

6.1.1 Disturbance Profile 2

As mentioned earlier the speed of the machine will increase with an increasing voltage, which can be seen in Figure 6-1. The slip will thus decrease and the rotor impedance increase, with a lower rotor current as result. More current will thus flow through the magnetizing part. However the total current consumed is decreased compared to pre fault, Figure 6-2. The increase of the magnetizing current will be presented later in Figure 6-9.

Due to the increased magnetizing current the motor will consume more reactive power, Figure 6-3, the change in active power is tiny. In Figure 6-4 the torque ripple due to the sudden increase of voltage can be seen.

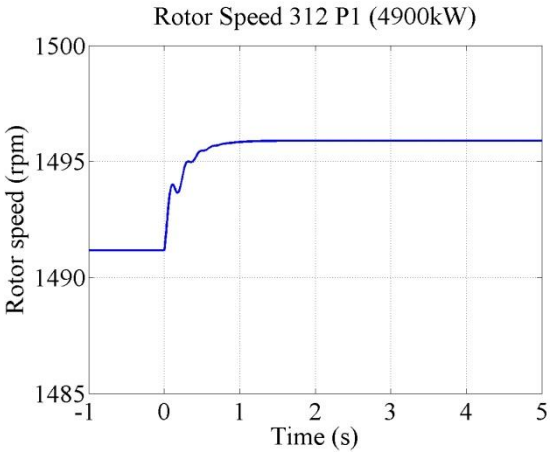

Figure 6-1: The increase in speed due to a voltage increase according to Disturbance Profile 2.

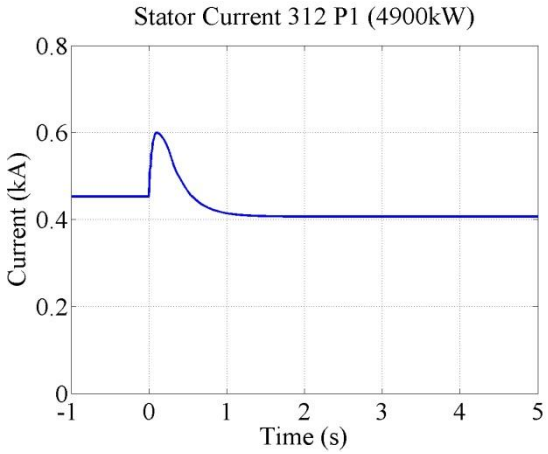

Figure 6-2: Resulting current.

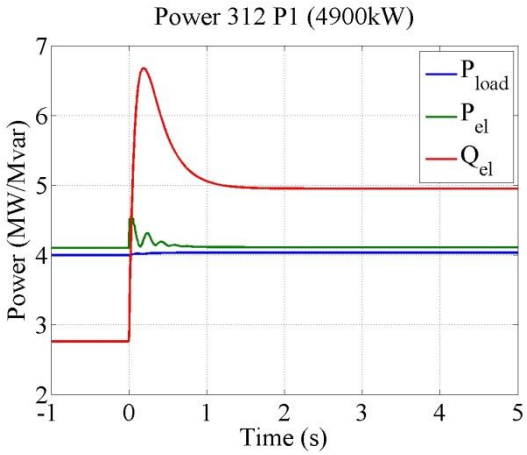

Figure 6-3: Resulting powers.

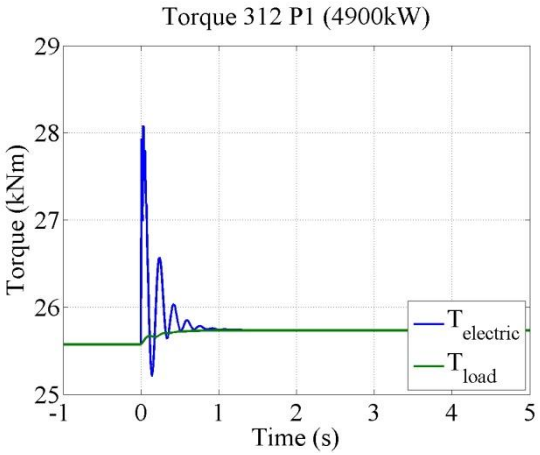

Figure 6-4: Resulting torques.

6.2 Saturation considered

This section presents the response of asynchronous machines, with saturation considered. The constant value of the magnetizing inductance used in previous chapters is exchanged for the current dependent inductance presented in Section 2.2.

6.2.1 Disturbance Profile 2

Compared with the results in Section 6.1.1, where no saturation is considered, the variation in speed and torque is almost the same. For the 4900 kW machine the speed increases from the initial speed of 1492 rpm to 1496 rpm and the ripple in the electrical torque has a maximum peak of 27.02 kNm, which not exceeds the rated torque of 31.42 kNm and should not expose the motor for any risk of damage.

When looking at the current in Figure 6-6 it can be seen that the current after the load rejection is increased instead of decreased when saturation is considered, this is what happens when the inductance becomes saturated. When a voltage is applied to the motor the magnetic field is increased and the magnetic domains in the iron core start to align. When a higher

voltage is applied, the motor draws a higher current in an attempt to magnetize the core over the level to which it easily can be magnetized.

The stator current increases from 90.7 to 104.5 percent of rated current. The higher current results in a higher reactive power due to the magnetization of the iron core.

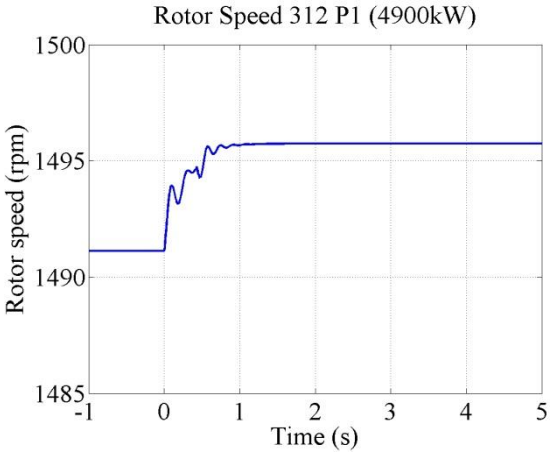

6-5: The variation in speed when the voltage is increased due to load rejection.

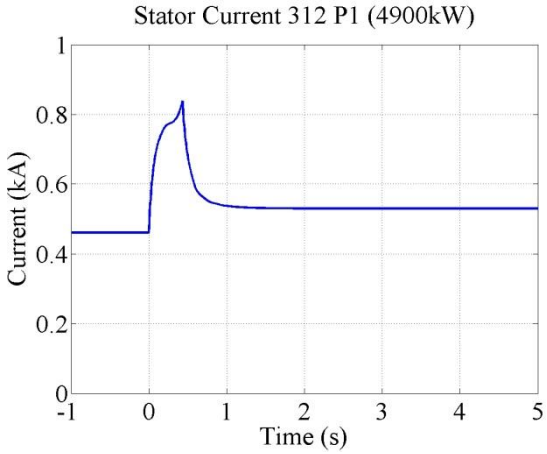

6-6: Resulting stator current.

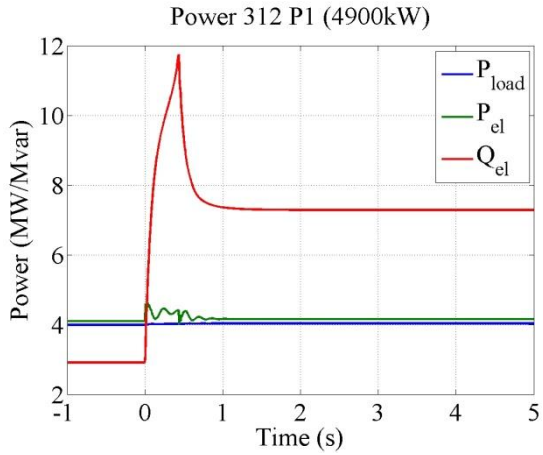

6-7: The variation in active and reactive power.

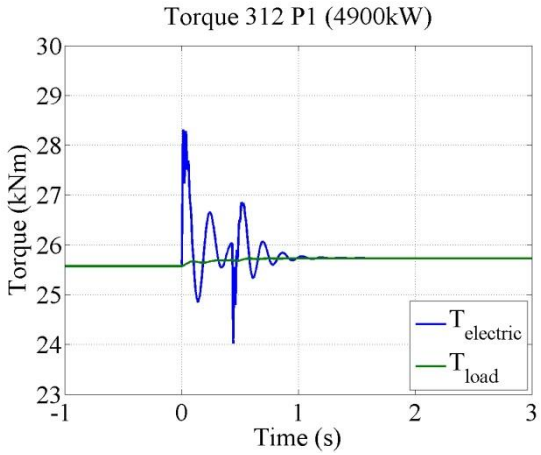

6-8: The torque ripple that the machine is exposed to during the increase in voltage.

In Table 6-1, numerical values from Figure 6-5 to 6-8 are presented for specified moments.

Table 6-1: Numerical values from specified moments of the simulation of the 4900 kW machine exposed to an increase of voltage according to Disturbance Profile 2.

Time (s)	Voltage (pu)	Current (kA)	Speed (rpm)	P_{load} (MW)	P_{el} (MW)	Q_{el} (Mvar)	$T_{electric}$ (kNm)	T_{load} (kNm)
0.00	1.00	0.46	1491	3.99	4.10	2.91	25.57	25.57
0.01	1.02	0.52	1491	3.99	4.57	3.50	28.31	25.58
0.10	1.15	0.70	1494	4.01	4.27	7.70	25.66	25.67
0.20	1.25	0.76	1493	4.01	4.37	9.40	26.11	25.64
0.35	1.34	0.79	1495	4.02	4.30	10.68	25.56	25.69
0.43	1.37	0.84	1495	4.02	4.42	11.74	26.03	25.69
0.68	1.42	0.57	1495	4.03	4.22	7.68	26.02	25.71
1.87	1.45	0.53	1496	4.03	4.15	7.29	25.73	25.73

In Figure 6-9 the magnetizing current during the load rejection according to Disturbance Profile 2 is presented, both when saturation is considered and not. For the first case the current is increased twice as much as in the second case when saturation is not considered. In Figure 6-10 it can be noted that the high current is caused by the fact that the magnetizing inductance saturates when the current increases. Since the current dependent inductance function is extrapolated from calculations on a 15 kW machine, the inductance has maximum and minimum limitations corresponding to the measured region. In the figure it is seen that the inductance adopts the value of the lower limit before the voltage has reached its end value. However, it gives a feeling of how the machine is affected by saturation.

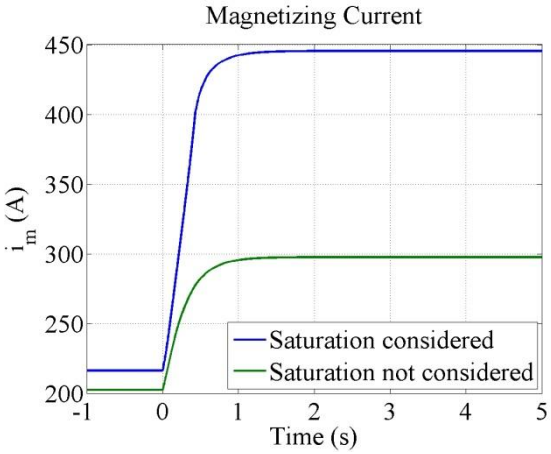

6-9: The magnetizing current in the 4900 kW machine during the load rejection, both when saturation is considered and not.

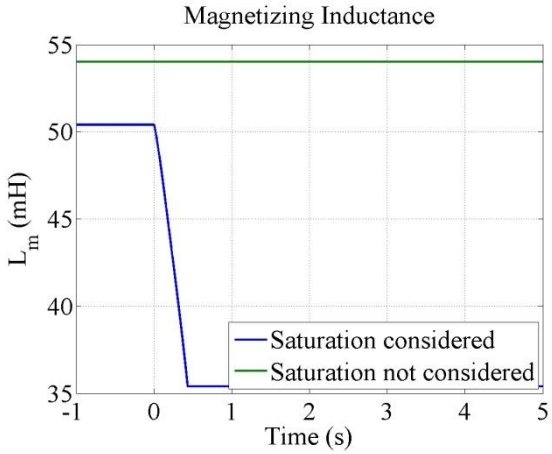

6-10: The magnetizing inductance in the 4900 kW machine during the load rejection, both when saturation is considered and not.

In Figure 6-11 – 6-14 the result from the same simulations of the 350 kW machine is presented. The machine is acting in the same way as the previous one. The speed increases from 2966 to 2984 rpm and the current increases from 89.9 to 101.4 percent of rated. The reactive power consumed by the machine is increased from 192 to 505 kvar. The torque ripple has a maximum peak of 1060 Nm, which can be compared to the rated torque of 1130 Nm.

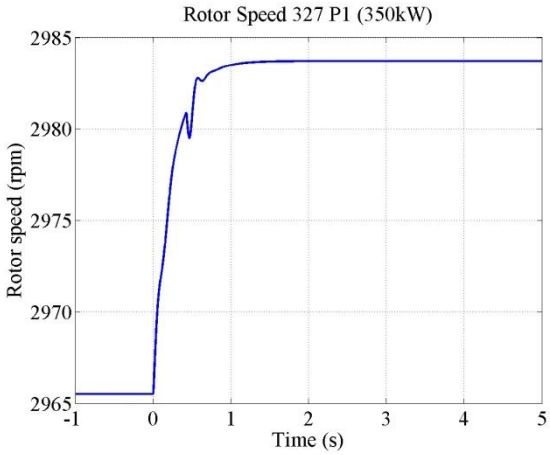

6-11: The variation in speed for the 350 kW machine when exposed to the voltage increase according to Disturbance Profile 2.

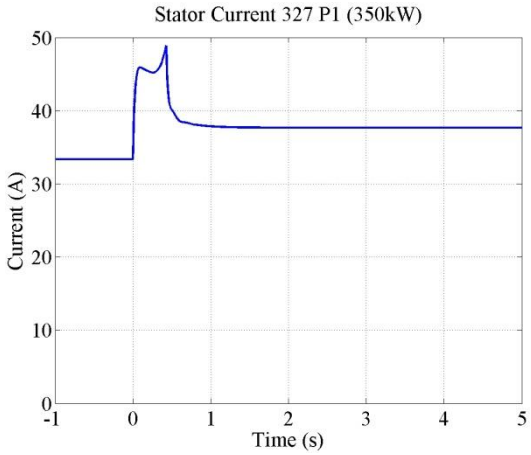

6-12: The current variation of the 350 kW machine.

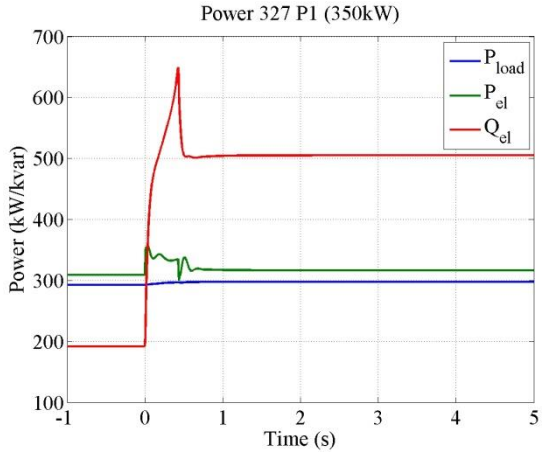

6-13: The corresponding power consumption of the 350 kW machine.

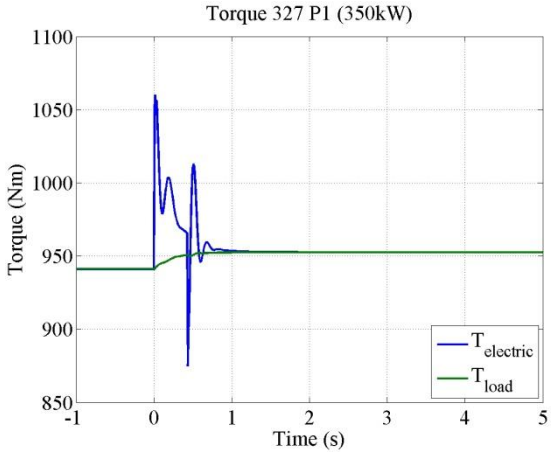

6-14. The torque variation of the 350 kW machine.

As can be seen in Figure 6-16 the magnetizing inductance reaches the lower limit also for the 350 kW motor.

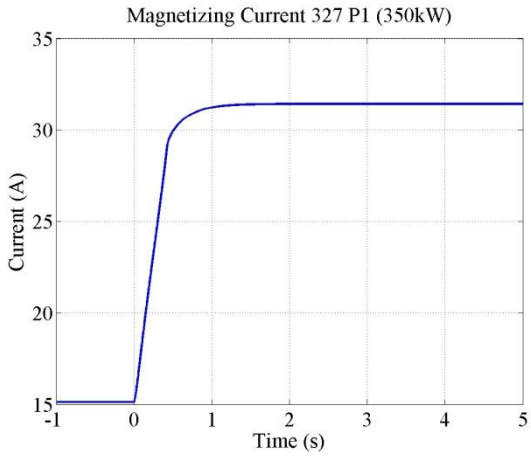

6-15: Magnetizing current in the 350 kW machine during a load rejection according to Disturbance Profile 2.

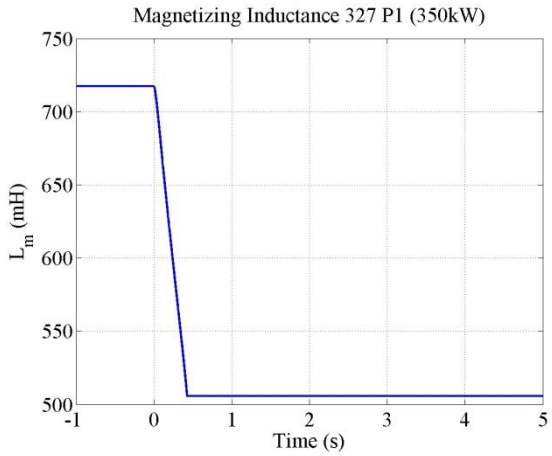

6-16: The corresponding magnetizing inductance.

Figure 6-17 – 6-20 presents the response of the 90 kW asynchronous machine when it experience the load rejection according to Disturbance Profile 2. The speed increases from 1480 to 1490 rpm. The current increases from 85 to 129 percent, which means that there can be problems with overheating if the voltage is not decreased in time. The reactive power consumption is highly increased from 68.9 to 200.6 kvar and the torque ripple has a maximum peak of 575.5 Nm which is close to the rated torque of 580 Nm.

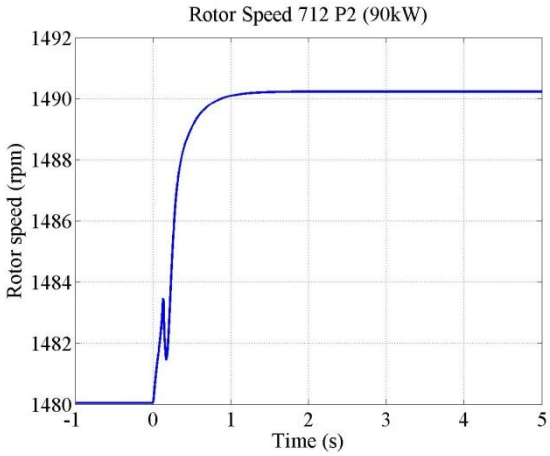

6-17: The variation in speed for the 90 kW machine when exposed to the voltage increase according to Disturbance Profile 2.

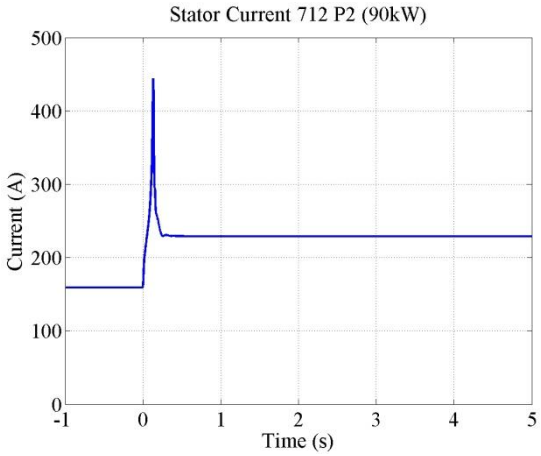

6-18: The current increase during the load rejection.

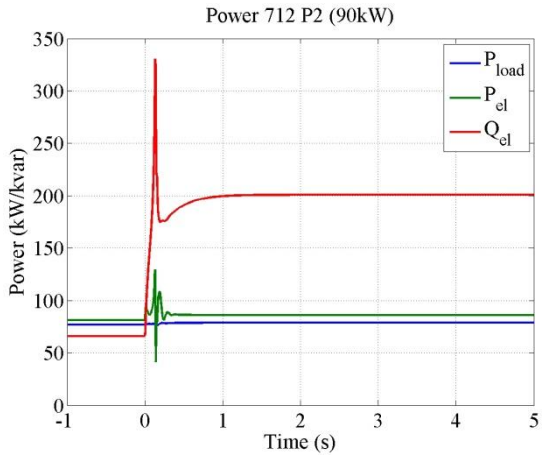

6-19: Power consumption.

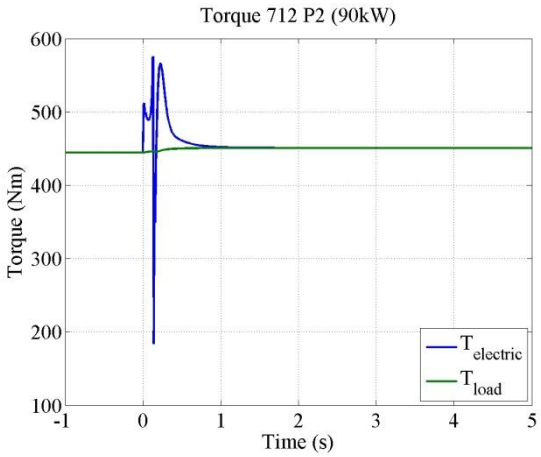

6-20: The change in torque.

In Figure 6-21 and 6-22 the magnetizing current and inductance is presented. Also for this machine the inductance reaches the lower limit.

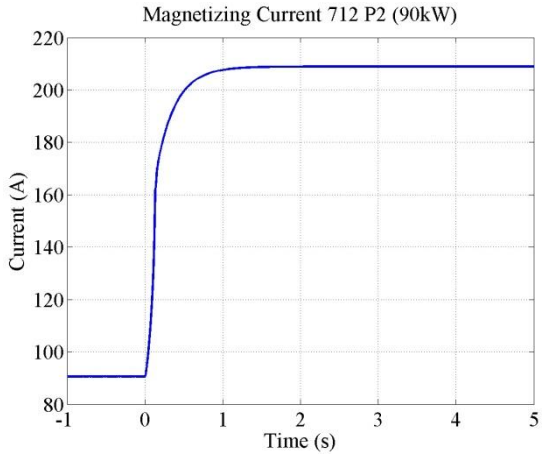

6-21 Magnetizing current in the 90 kW machine during a load rejection according to Disturbance Profile 2.

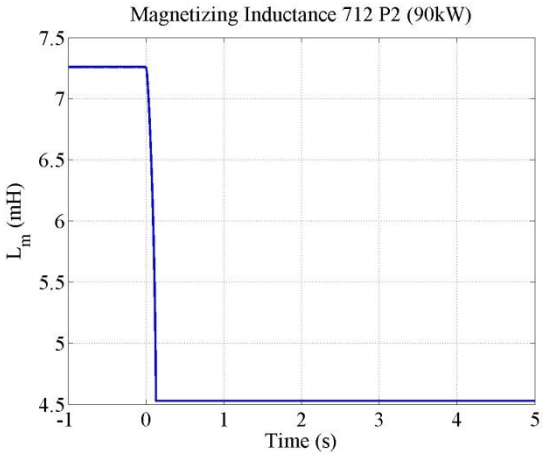

6-22: The corresponding magnetizing inductance.

6.2.2 Disturbance Profile 5

The speed variation of the 4900 kW machine during a three phase voltage dip according to Disturbance Profile 5 is shown in Figure 6-23. Before the voltage dip occurs, the machine is in steady state and has a speed of 1491 rpm. When the dip occurs the speed decreases with 8.5 percent to 1365 rpm. After the dip, the voltage is not fully recovered, only to 95 percent, and the machine is accelerating to a new steady state speed of 1490 rpm. Since it takes some milliseconds to build up the airgap field from that the voltage starts to recover the speed continues to decrease, even after the voltage is recovered, before it increases.

The machine is loaded so that the current is at rated level when the voltage is decreased to a level of 85 percent of rated. When the voltage dip is initialized there is a current transient of 3.47 kA and subsequently it reaches a level of 142 percent of rated during the dip. When the voltage recovers there is a high inrush current to first build up the airfield and then to accelerate the motor. It has a maximum phase rms value of 389.5 percent of rated and lasts for approximately 0.7 seconds. When the voltage has recovered, the stator current has a value of 473.6 A, 93.4 percent of rated.

In Figure 6-25 the active and reactive electric power, P_{el} and Q_{el}, are presented together with power demand of the load, P_{load}. The mechanical output power is slightly lower than the electrical input power due to losses in the machine. When the voltage dips, both active and reactive power decreases and becomes negative due to the machine is moving from motor to generator mode during the deceleration. When the voltage recovers and the machine is accelerating the active and reactive power is increasing. The reactive power increases due to the magnetization of the machine and reaches a top value of 16.51 Mvar, 567 percent of the power consumed before the voltage dip (2.91 Mvar). Then it decreases to the new steady state of 2.69 Mvar.

In Figure 6-26 the torque oscillations can be seen when the voltage dip occurs and when it recovers. The load torque is decreased during the dip due to the speed dependence.

During the voltage dip the magnetizing current is not increased and there is no risk that the magnetizing inductance will saturate.

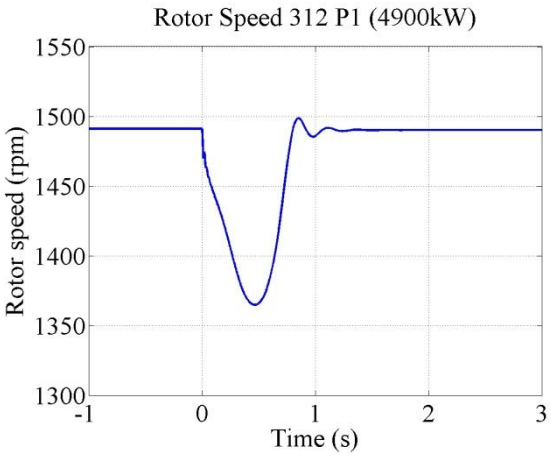

Figure 6-23: Motor speed variation of the 4900 kW machine as function of time for a voltage dip according to Disturbance Profile 5.

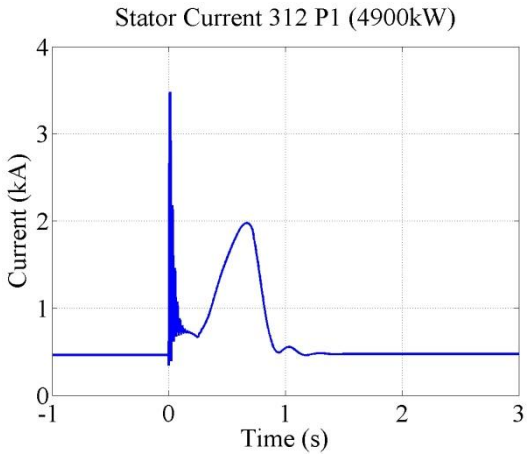

Figure 6-24: Stator current variation for a voltage dip according to Disturbance Profile 5.

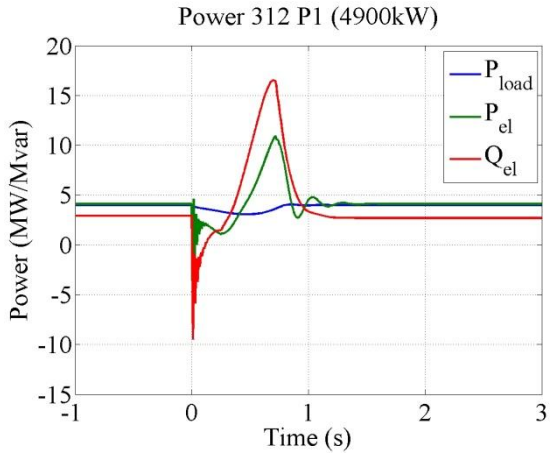

Figure 6-25: Electrical, mechanical and load power for a voltage dip according to Disturbance Profile 5.

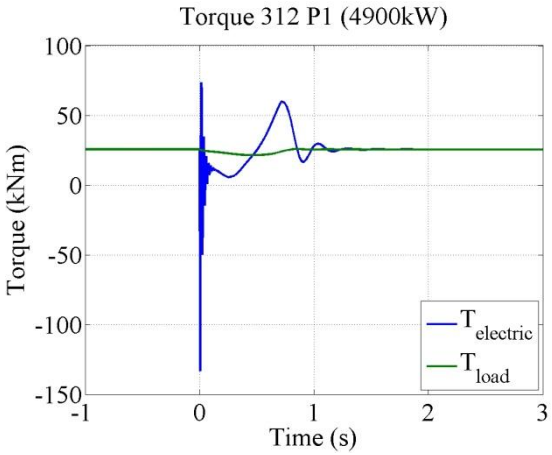

Figure 6-26: Electrical and load torque for a voltage dip according to Disturbance Profile 5.

In Table 6-2 numerical values from the figures above can be seen at specific times.

Table 6-2: Numerical values from specified moments of the simulation of the 4900 kW machine exposed to a voltage dip according to Disturbance Profile 5.

Time (s)	Voltage (pu)	Current (kA)	Speed (rpm)	P_{load} (MW)	P_{el} (MW)	Q_{el} (Mvar)	$T_{electric}$ (kNm)	T_{load} (kNm)
0.00	1.00	0.46	1491	3.99	4.10	2.91	25.57	25.57
0.01	0.25	3.47	1491	3.84	4.63	-3.62	73.49	25.57
0.15	0.25	0.72	1434	3.55	1.85	0.71	10.2	23.64
0.25	0.25	0.66	1405	3.34	1.06	1.47	5.60	22.71
0.46	0.57	1.41	1365	3.06	4.13	7.79	20.73	21.42
0.66	0.86	1.98	1409	3.37	9.55	16.00	50.49	22.83
0.70	0.95	1.95	1432	3.54	10.63	16.51	57.67	23.58
0.72	0.95	1.83	1445	3.63	10.92	16.26	60.06	24.01
0.85	0.95	0.75	1499	4.05	4.35	6.71	25.83	25.83
1.60	0.95	0.47	1490	3.98	4.09	2.68	25.54	25.54

In Figure 6-27 – 6-30 the response of the 350 kW machine is presented when exposed to the voltage dip according to Disturbance Profile 5. It behaves more or less in the same way as the previous machine.

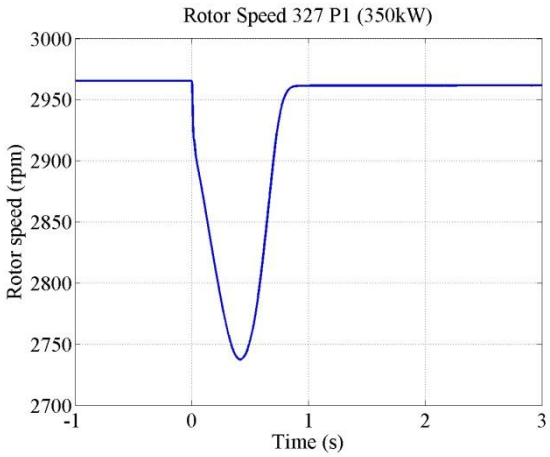

Figure 6-27: Motor speed variation of the 350 kW machine as a function of time for a voltage dip according to Disturbance Profile 5.

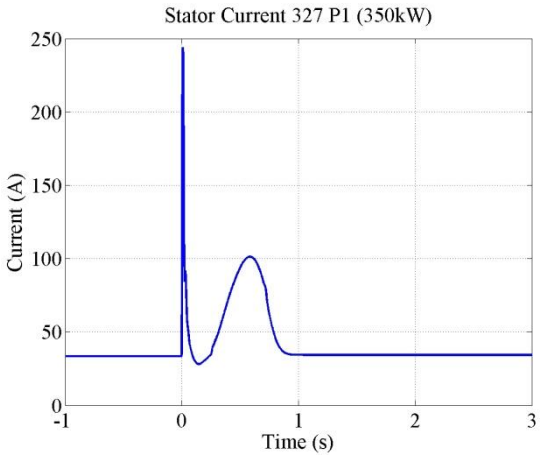

Figure 6-28: Stator current variation for a voltage dip according to Disturbance Profile 5.

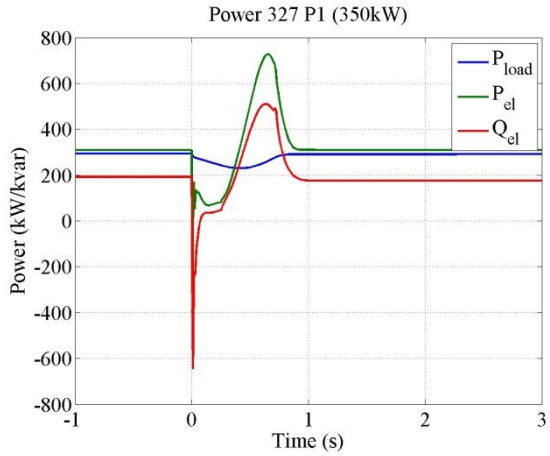

Figure 6-29: Electrical, mechanical and load power for a voltage dip according to Disturbance Profile 5.

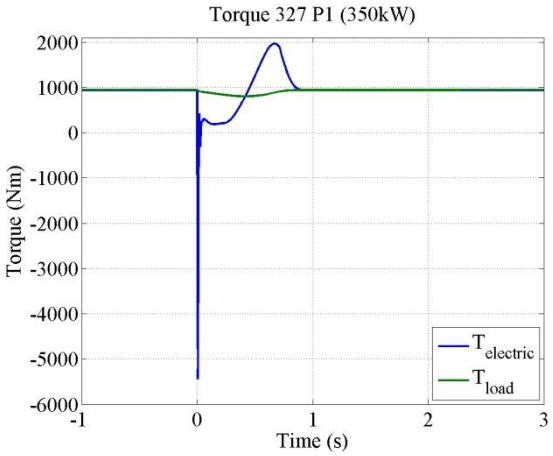

Figure 6-30: Electrical and load torque for a voltage dip according to Disturbance Profile 5.

In Figure 6-31 – 6-34 the response of the 90 kW machine is presented when exposed to the voltage dip according to Disturbance Profile 5.

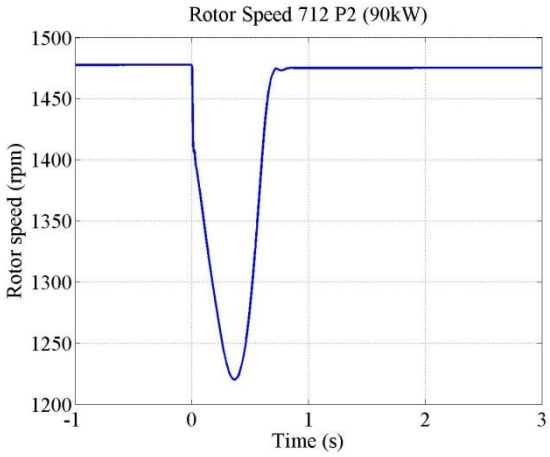

Figure 6-31: Motor speed variation of the 90 kW machine as a function of time for a voltage dip according to Disturbance Profile 5.

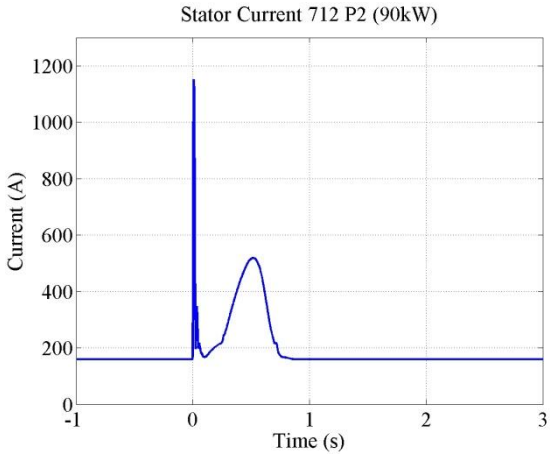

Figure 6-32: Stator current variation for a voltage dip according to Disturbance Profile 5.

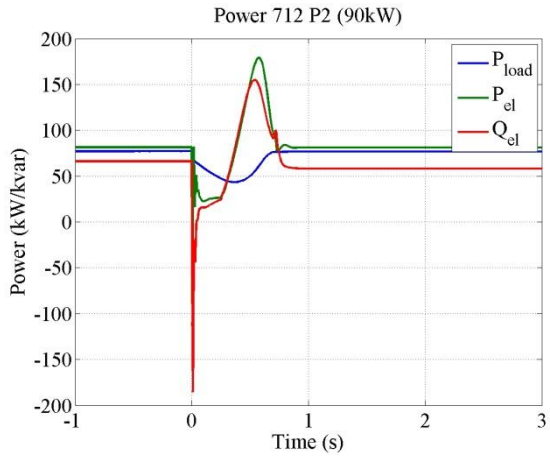

Figure 6-33: Electrical, mechanical and load power for a voltage dip according to Disturbance Profile 5.

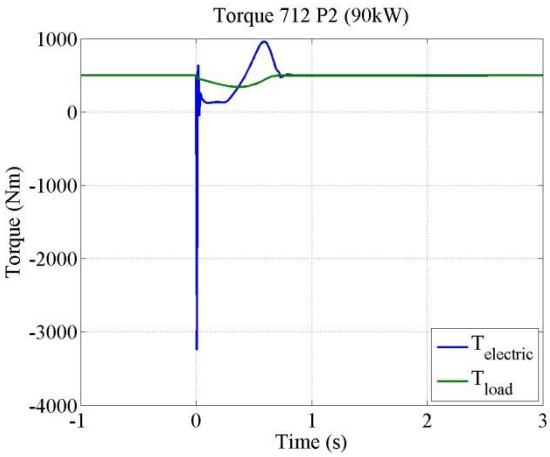

Figure 6-34: Electrical and load torque for a voltage dip according to Disturbance Profile 5.

6.2.3 Disturbance Profile 7

When the voltage dip occurs, the speed of the 4900 kW machine is decreased with 11.3 percent, from 1491 to 1322 rpm. When the field in the air gap is build up it accelerates and after the swell it reaches a speed of 1492 rpm due to the slightly higher stator voltage.

Figure 6-36 shows current variations during the dip and the swell according to Disturbance Profile 7. During the dip the current rises to 130.1 percent and afterwards it increases rapidly to 507.0 percent for around half a second and then reaches a new steady state value of 88.7 percent. During the swell the current is somewhat lower. Unlike Disturbance Profile 2 where the current increased when a higher voltage was applied, the current is decreases due to no saturation of the magnetizing inductance.

In Figure 6-37 the consumption of active and reactive power is presented.

Figure 6-38 shows the variation in torque during the dip and swell. The typical torque transient can be seen when the voltage dip occurs as well as the increased power demand during the acceleration due to higher inrush current.

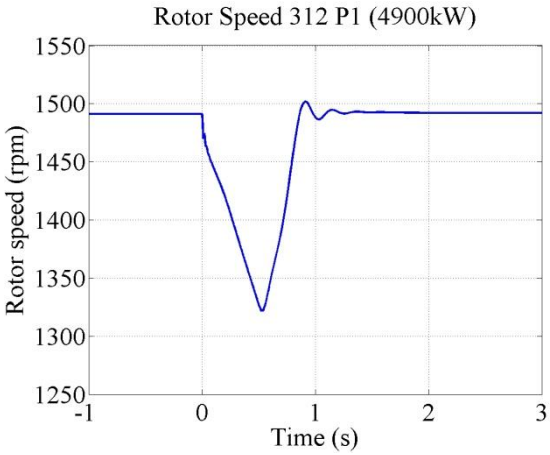

Figure 6-35: Motor speed variation of the 4900 kW machine as a function of time for a voltage dip according to Disturbance Profile 7.

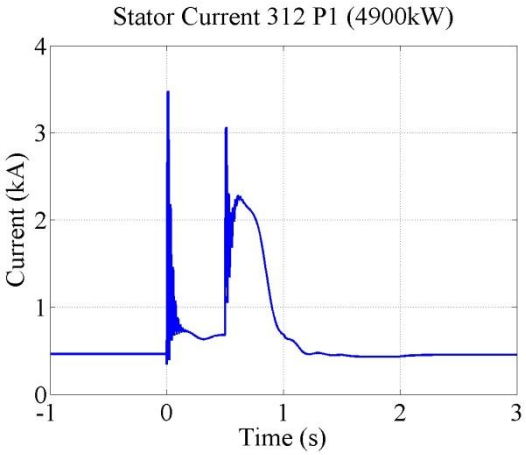

Figure 6-36: Stator current variation for a voltage dip according to Disturbance Profile 7.

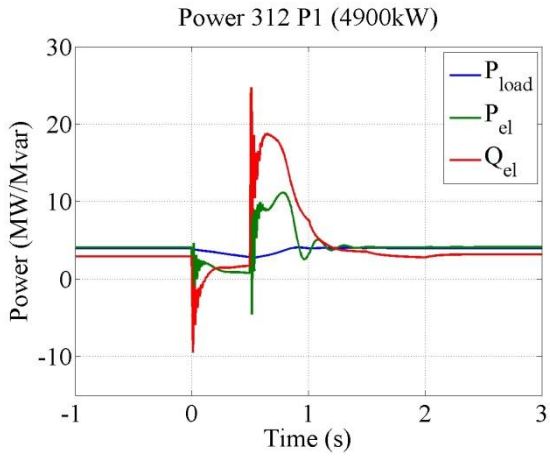

Figure 6-37: Electrical, mechanical and load power for a voltage dip according to Disturbance Profile 7.

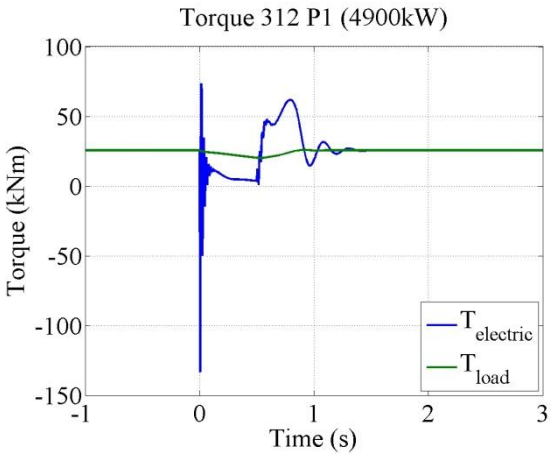

Figure 6-38: Electrical and load torque for a voltage dip according to Disturbance Profile 7.

In Table 6-3 numerical values of specified moments of the simulation can be seen.

Table 6-3: Numerical values from specified moments of the simulation of the 4900 kW machine exposed to a voltage dip followed by a swell according to Disturbance Profile 7.

Time (s)	Voltage (pu)	Current (kA)	Speed (rpm)	P_{load} (MW)	P_{el} (MW)	Q_{el} (Mvar)	$T_{electric}$ (kNm)	T_{load} (kNm)
0.00	1.00	0.46	1491	3.99	4.10	2.91	25.57	25.57
0.01	0.25	3.48	1471	3.83	4.63	-9.48	73.49	24.96
0.10	0.25	0.74	1445	3.64	2.06	-0.27	12.94	24.03
0.25	0.25	0.66	1405	3.34	1.06	1.47	5.60	22.71
0.51	0.75	2.57	1322	2.80	3.31	24.75	8.15	20.19
0.61	0.83	2.27	1350	2.97	9.24	18.38	46.10	20.97
0.65	0.86	2.22	1367	3.08	8.91	18.77	44.15	21.50
0.79	0.95	1.86	1447	3.65	11.12	16.04	61.75	24.08
1.01	1.10	0.66	1487	3.96	3.37	7.22	20.41	25.44
1.40	1.10	0.45	1493	4.01	4.02	3.59	25.09	25.63
1.75	1.08	0.43	1492	4.00	4.10	2.96	25.58	25.61
2.50	1.05	0.45	1492	4.00	4.10	3.18	25.60	25.60

Figure 6-39 – 6-42 shows the response of the 350 kW machine when simulations of Disturbances Profile 7 is performed.

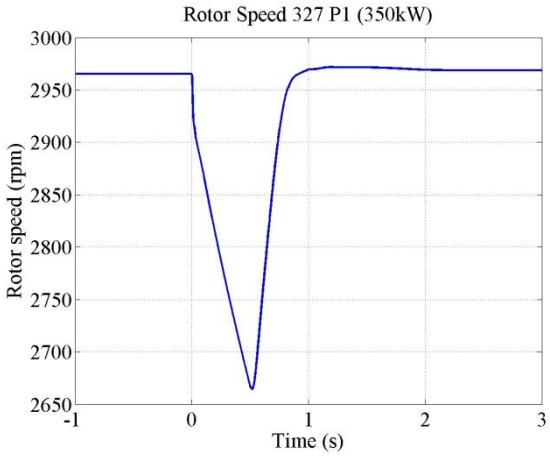

Figure 6-39: Motor speed variation of the 350 kW machine as a function of time for a voltage dip according to Disturbance Profile 7.

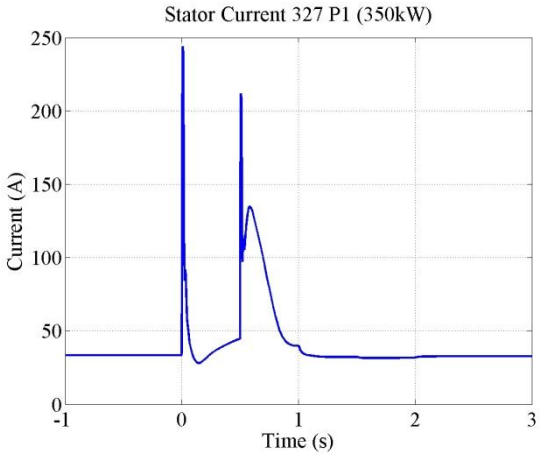

Figure 6-40: Stator current variation for a voltage dip according to Disturbance Profile 7.

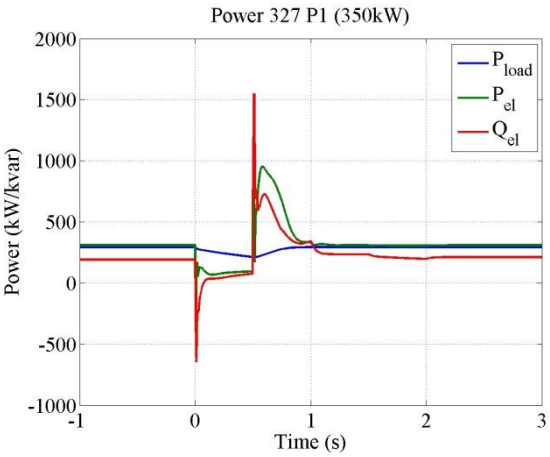

Figure 6-41: Electrical, mechanical and load power for a voltage dip according to Disturbance Profile 7.

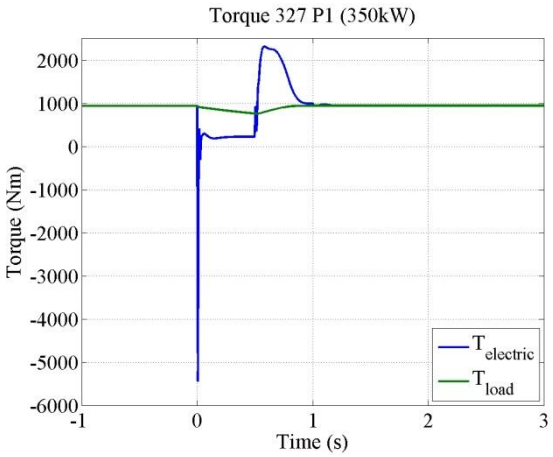

Figure 6-42: Electrical and load torque for a voltage dip according to Disturbance Profile 7.

Figure 6-43 – 6-46 shows the response of the 90 kW machine when simulation of Disturbances Profile 7 is performed.

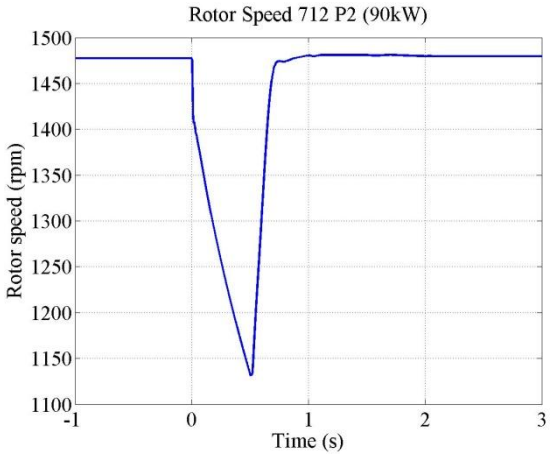

Figure 6-43: Motor speed variation of the 90 kW machine as function of time for a voltage dip according to Disturbance Profile 7.

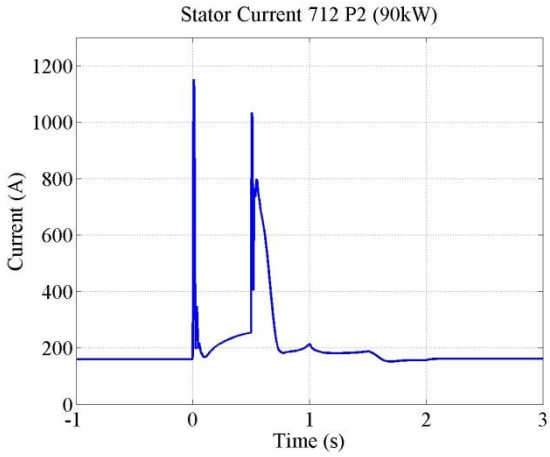

Figure 6-44: Stator current variation for a voltage dip according to Disturbance Profile 7.

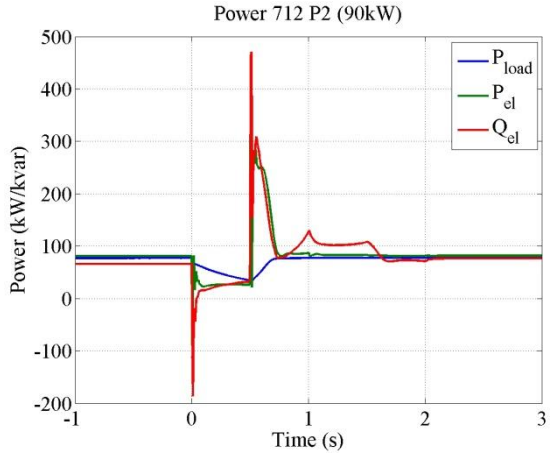

Figure 6-45: Electrical, mechanical and load power for a voltage dip according to Disturbance Profile 7.

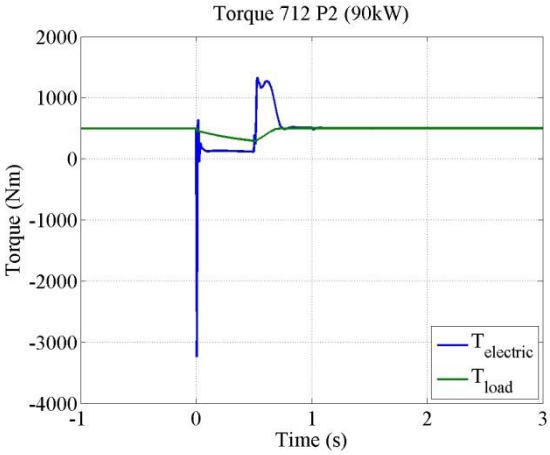

Figure 6-46: Electrical and load torque for a voltage dip according to Disturbance Profile 7.

6.2.4 Disturbance Profile 12

Like previous, the 4900 kW machine is assumed to be loaded to a level where the machine is consuming rated current at a voltage level of 85 percent of rated. In that operational case the machine is running at a speed of 1491 rpm. The frequency variation is not of high interest according to OKG, therefore it has been neglected.

As described in Chapter 3 the machine will decelerate when the voltage decreases. This can also be seen in Figure 6-51 where the machine torque, calculated from the voltages in Disturbance Profile 12, is presented together with the load torque of pump characteristics. The figure also clearly shows the fact that the synchronous speed, as it is decreasing with the frequency, will speed up the deceleration of the machine.

While the voltage is decreasing the current is increasing to maintain the power. When the voltage after five minutes has decreased to 85 percent the current is reaching the rated level.

After another five minutes the voltage has decreased to 70 percent and the current has increased to 120.9 percent. At this point the machine has a speed of 1480 rpm.

When looking at Figure 6-51 with the stability criterion from Section 2.3.3 in the mind, it is clear that the machine in this case is running in stable operation. However, the machine is heavily loaded and the current is high which leads to temperature problems.

When the rate of change of voltage increases and the frequency starts to fall the machine becomes highly overloaded and, if the machine is not yet switched off due to temperature problems, it will soon or later stall due to insufficient electro dynamical driving torque.

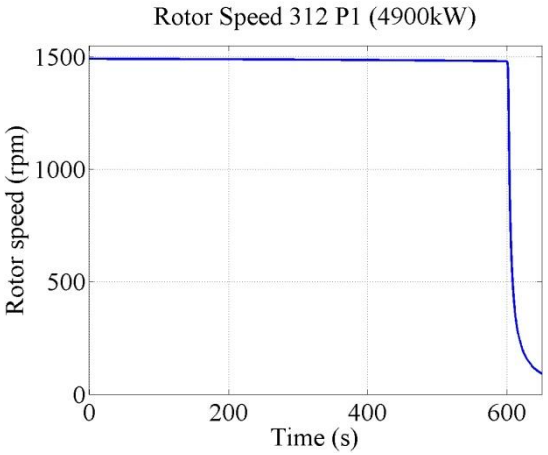

6-47: Motor speed variation of the 4900 kW machine as a function of time during a voltage collapse according to Disturbance Profile 12.

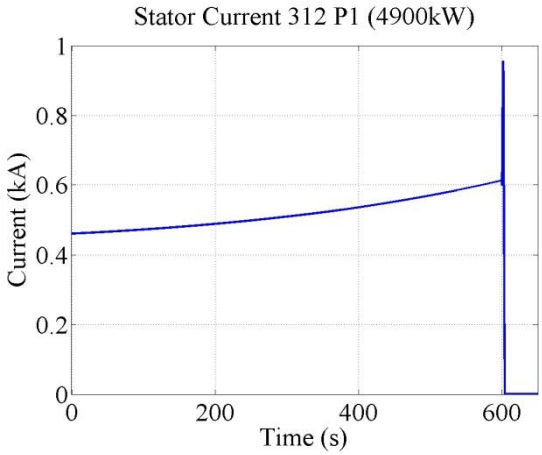

6-48: Stator current variation during a voltage collapse according to Disturbance Profile 12.

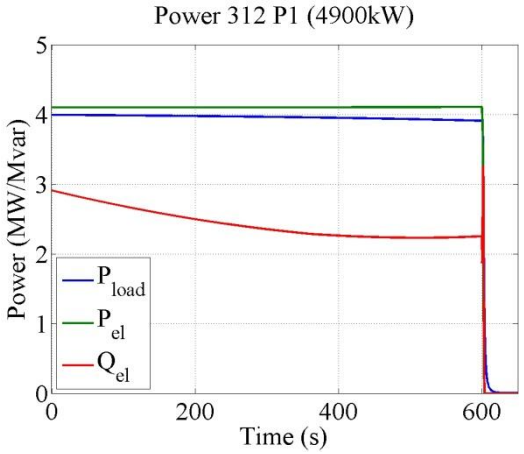

6-49: Electrical, mechanical and load during a voltage collapse according to Disturbance Profile 12.

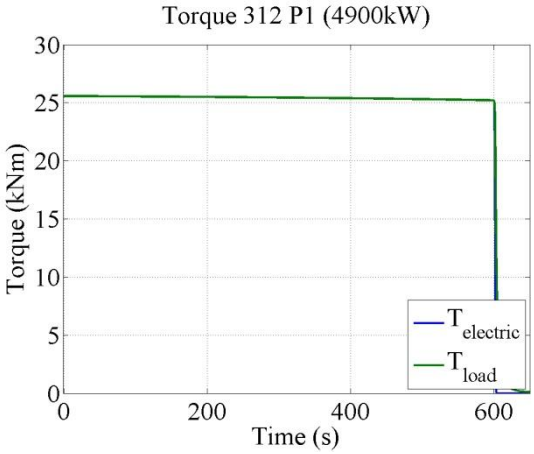

6-50: Electrical and load torque during a voltage collapse according to Disturbance Profile 12.

In Table 6-4 numerical values from the simulation above can be found.

Table 6-4: Numerical values from specified moments of the simulation of the 4900 kW machine during a voltage collapse according to Disturbance Profile 12.

Time (s)	Voltage (pu)	i_s (A)	n (rpm)	P_{load} (MW)	P_{el} (MW)	Q_{el} (Mvar)	$T_{electric}$ (kNm)	T_{load} (kNm)
0	1.00	460.76	1491.6	3.99	4.100	2.91	25.57	25.57
100	0.95	472.56	1490.1	3.98	4.099	2.68	25.53	25.53
200	0.90	488.70	1488.9	3.97	4.098	2.50	25.49	25.49
300	0.85	509.52	1487.5	3.96	4.099	2.35	25.44	25.44
400	0.80	536.36	1485.7	3.94	4.100	2.26	25.38	25.38
500	0.75	570.58	1483.4	3.93	4.103	2.23	25.30	25.30
600	0.70	613.18	1480.4	3.91	4.107	2.25	25.20	25.20

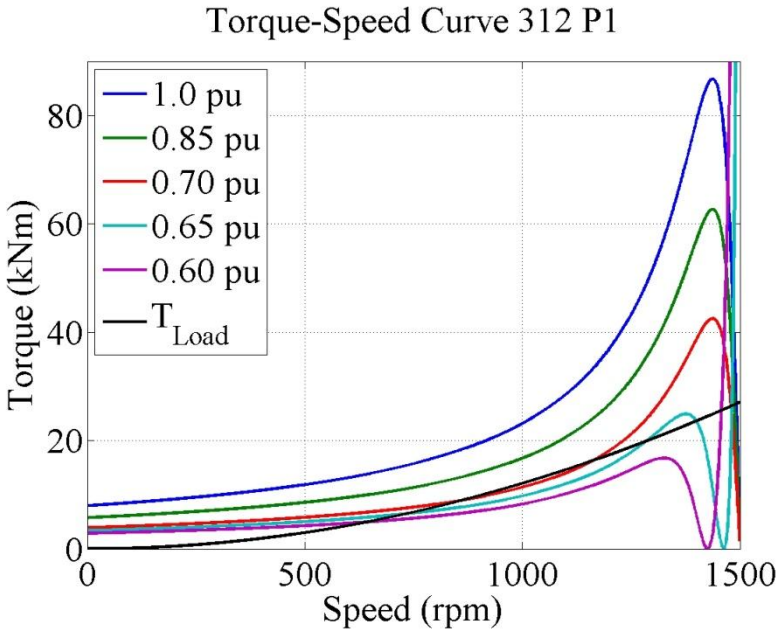

Figure 6-51: Machine torques at different voltages together with the load torque during the voltage collapse according to Disturbance Profile 12

In Figure 6-52 – 6-55 the response of the 350 kW machine is presented.

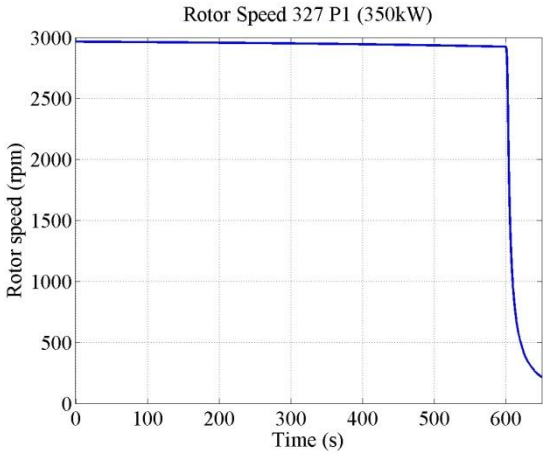

Figure 6-52: Motor speed variation of the 350 kW machine as a function of time during a voltage collapse according to Disturbance Profile 12.

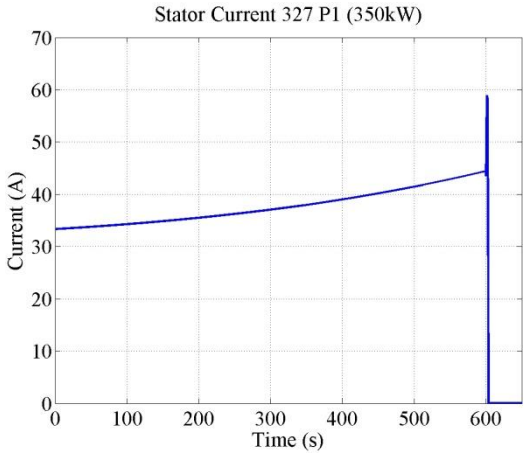

Figure 6-53: Stator current variation during a voltage collapse according to Disturbance Profile 12.

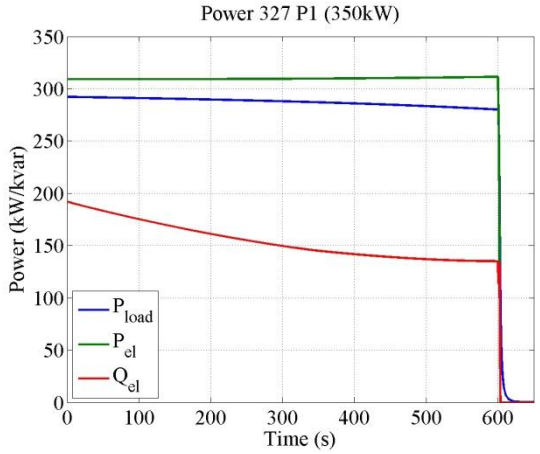

Figure 6-54: Electrical, mechanical and load during a voltage collapse according to Disturbance Profile 12.

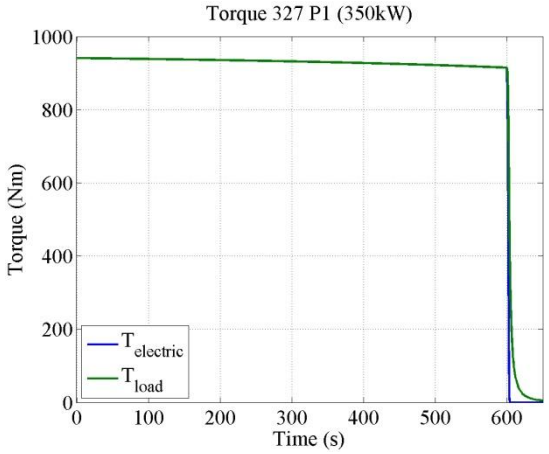

Figure 6-55: Electrical and load torque during a voltage collapse according to Disturbance Profile 12.

In Figure 6-56 – 6-59 the response of the 90 kW machine is presented.

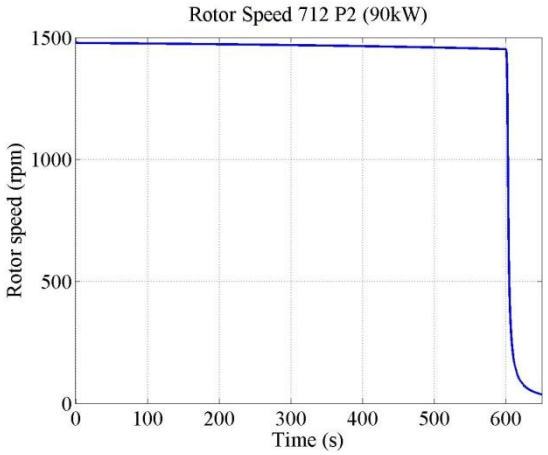

Figure 6-56: Motor speed variation of the 90 kW machine as a function of time during a voltage collapse according to Disturbance Profile 12.

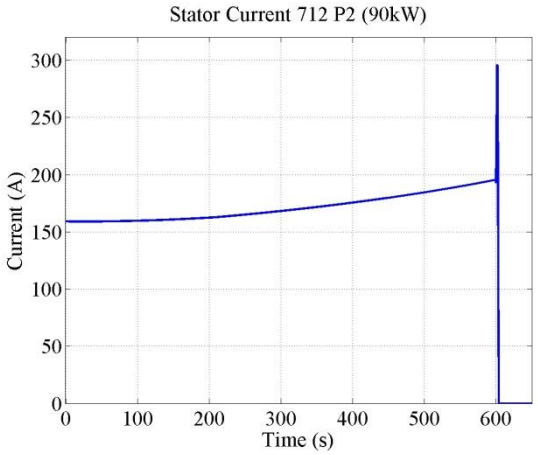

Figure 6-57: Stator current variation during a voltage collapse according to Disturbance Profile 12.

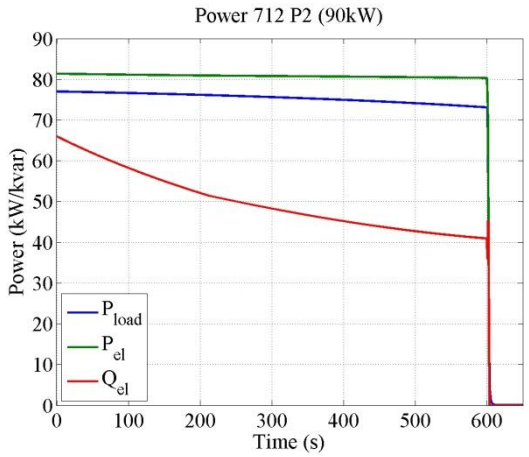

Figure 6-58: Electrical, mechanical and load during a voltage collapse according to Disturbance Profile 12.

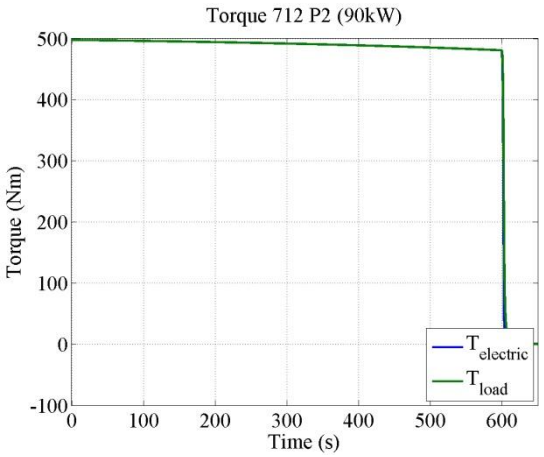

Figure 6-59: Electrical and load torque during a voltage collapse according to Disturbance Profile 12.

6.2.5 Disturbance Profile 13

To simplify the calculations of Disturbance Profile 13 when taking the frequency variation into account, static calculations of the stationary model in Figure 2-1 have been performed instead of dynamical simulations.

The 4900 kW machine is loaded in such a way that the machine consumes rated current at a voltage level of 85 percent. When the voltage dip is stabilized at 80 percent the stator current has increased from 90.7 to 106.7 percent of rated. At the same time the machine is decelerated and the slip increases from 0.0062 to 0.0101. When the frequency is increased from 50 Hz to 51 Hz the synchronous speed is increased from 1500 rpm to 1530 rpm. However, the slip is increased and therefore also the current is increased further to a level of 111.5 percent of rated current.

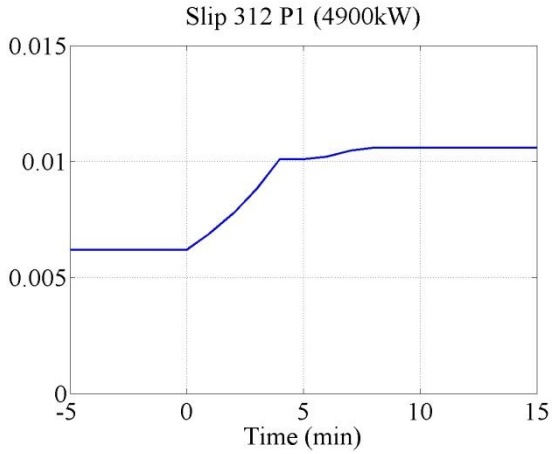

6-60: The variation in slip when the machine is exposed to a voltage dip according to Disturbance Profile 13.

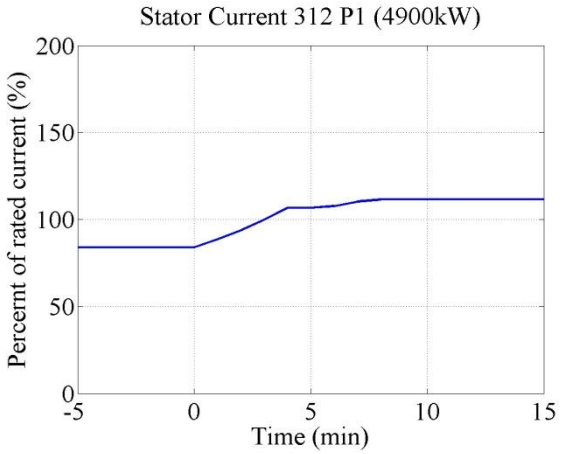

6-61: The increased use of current by the machine in percent of the rated current.

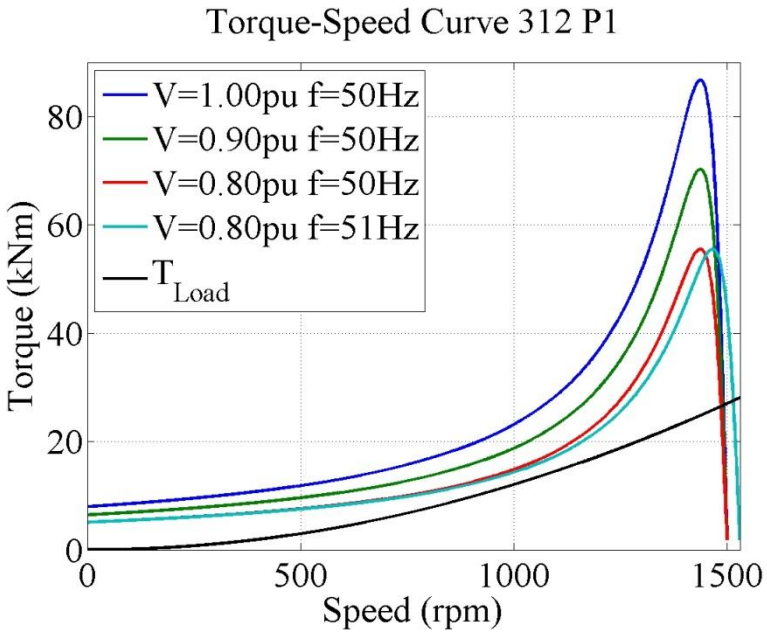

6-62: Torque speed curve at different operation points according to Disturbance Profile 13.

6.3 Trip Diagram

In Figure 6-63 to 6-65 trip diagrams of the investigated machines are presented. They were compiled by simulating voltage dips of different magnitude and duration and then comparing the resulting current with the thermal curve in Figure 3-3 to check if the machine would trip or not due to overheating.

The simulations were made when the machines were loaded with both 100 percent, blue rings, and 85 percent, red dots, of rated torque. The figures clearly show that a less loaded machine will withstand voltage dips of longer duration. For example, if the machine is running a load of 100 percent, it will withstand a voltage dip with a remaining voltage of 0.5 pu for 2.3 seconds. If the same machine is running a load of 85 percent it will instead withstand a voltage dip of the same magnitude for 3.0 seconds before getting overheated due to high currents. In all operation points under these points the machines will be overheated according to the thermal curve.

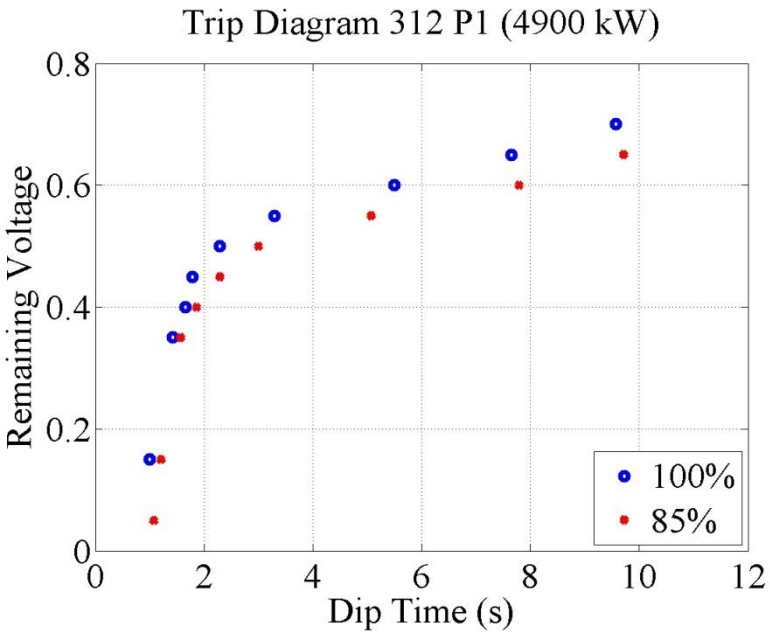

Figure 6-63: Trip diagram of the 4900 kW machine when exposed to voltage dips, of different magnitude and duration, loaded to 85 and 100 percent respectively.

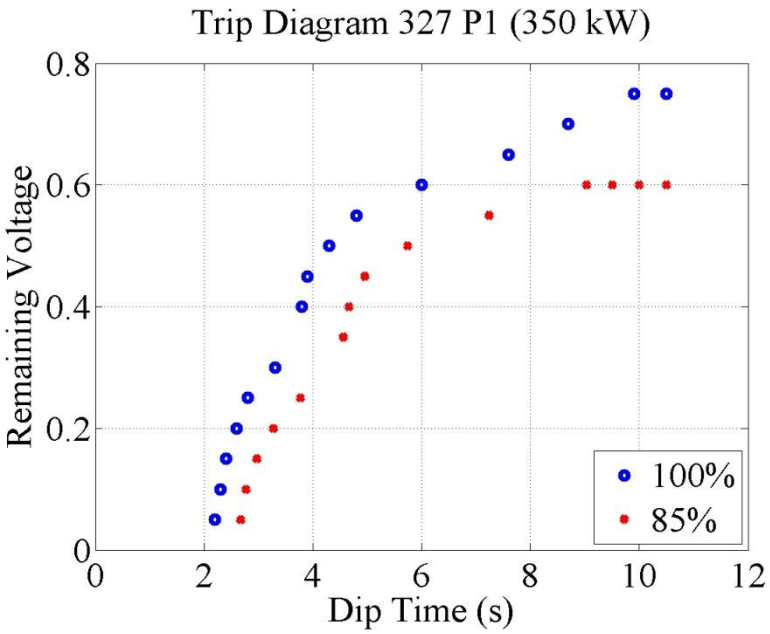

Figure 6-64: Trip diagram of the 350 kW machine when exposed to voltage dips, of different magnitude and duration, loaded to 85 and 100 percent respectively.

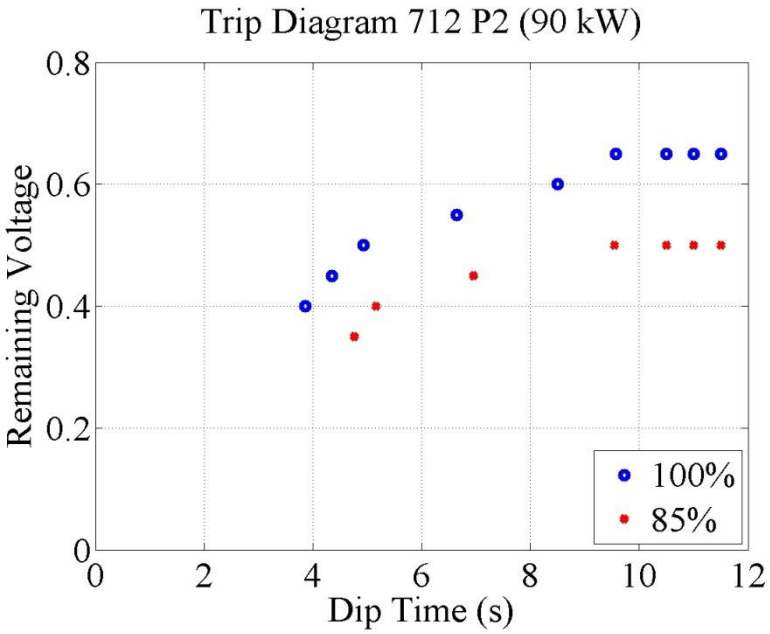

Figure 6-65: Trip diagram of the 90 kW machine when exposed to voltage dips, of different magnitude and duration, loaded to 85 and 100 percent respectively.

7 Measurements

This chapter contains the results from the measurements of the 4 kW machine at Chalmers. Machine parameters can be found in Appendix A. The results are compared to corresponding results from simulations of the machine in order to verify that the model used in previous chapters is correct.

The measured stator voltage contains a lot of disturbance components. Attempts have been made to filter it by a Butterworth filter, but without satisfactory result. Therefore the inverter is assumed to be strong enough to deliver a voltage level equal to the reference signal.

Also the signal from the speed measurements is extremely noisy, not even ferrites are enough to get rid of it.

The figures presented in the following tables are all, except the speed, from the measured values. From the noisy signals, a mean value is derived.

7.1 The speed-torque curve

In Figure 7-1the calculated torque-speed curve of the 4 kW machine, calculated in Section 2.3.1, is compared to the measured torque. During the measurements the machine was delta connected and fed through a 400/230 V transformer in order to not stress the machine. The torque was then extrapolated to a 400 V supply. As can be seen the model and the measurements are pretty consisting, at least in the operating region.

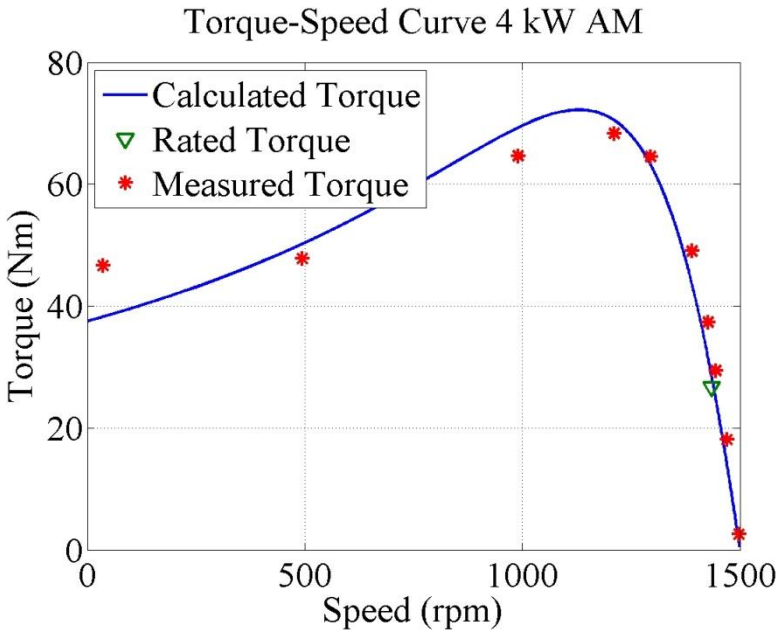

Figure 7-1: The measured and the calculated speed-torque curves of the 4 kW asynchronous machine.

7.2 Disturbance Profile 2

According to Disturbance Profile 2 the voltage increases to a level of 1.45 pu, unfortunately the test equipment at Chalmers only permitts a voltage level of 1.15 pu. Anyway, the results clearly shows how the machine is affected by overvoltages. Since the magnetizing inductance becomes saturated, the machine consumes a high magnetizing current and the reactive power consumption is increased with 63 percent altough the voltage level is only 1.15 pu.

The machine is loaded so that the machine consumes rated current at a voltage level of 85 percent of rated.

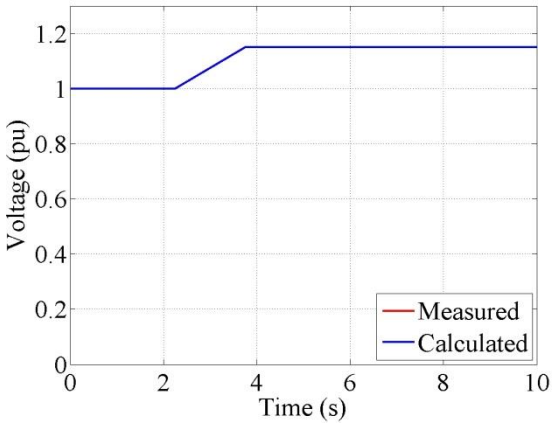

7-2: A variant of Voltage Profile 2.

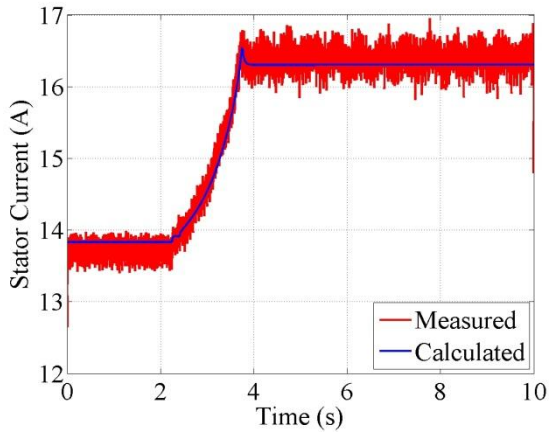

7-3: The calculated and measured stator current.

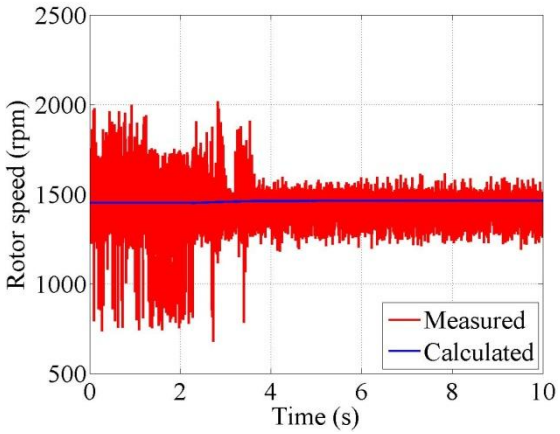

7-4: The calculated and measured speed variations.

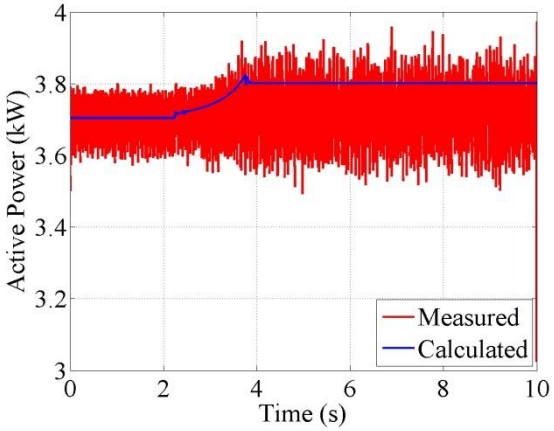

7-5: The calculated and measured active power.

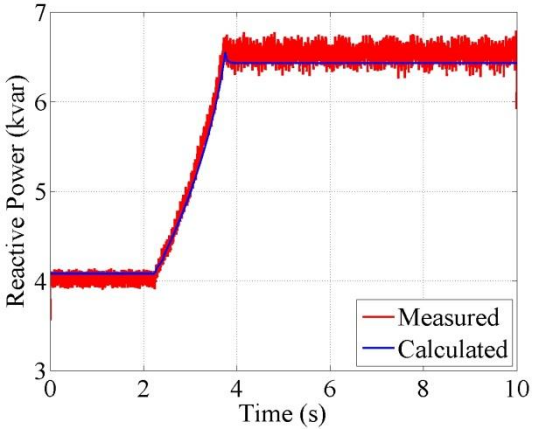

7-6: The calculated and measured reactive power.

In Table 7-1 the numerical value of the speed, current and power is presented for some specific moments during the test. It should be mentioned that these values are only valid for this specific machine.

Table 7-1: Disturbance Profile 2.

Time (s)	Voltage (pu)	Speed (rpm)	Current (A)	Active power (kW)	Reactive Power (kvar)
2.25	1.000	1450	13.66	3.70	4.02
2.50	1.025	1453	13.96	3.71	4.32
2.75	1.050	1455	14.36	3.72	4.70
3.00	1.075	1457	14.65	3.73	4.95
3.25	1.100	1459	15.06	3.74	5.47
3.50	1.125	1461	15.71	3.75	5.93
3.75	1.150	1462	16.75	3.75	6.54
4.00	1.150	1462	16.41	3.75	6.53

Before the voltage starts to increases the machine consumes a current of 86.5 percent of rated. When the voltage reaches a value of 1.15 pu the current consumption increases to 103.8 percent. At a voltage level of approximately 1.125 the current reaches rated current.

7.3 Disturbance Profile 5

The machine is loaded so that it consumes a current of approximately 11 A, which corresponds to 70 percent of rated. For higher loads the machine trips because the load torque exceeds the machine torque during the dip.

In the following figures the results from the measurements are presented.

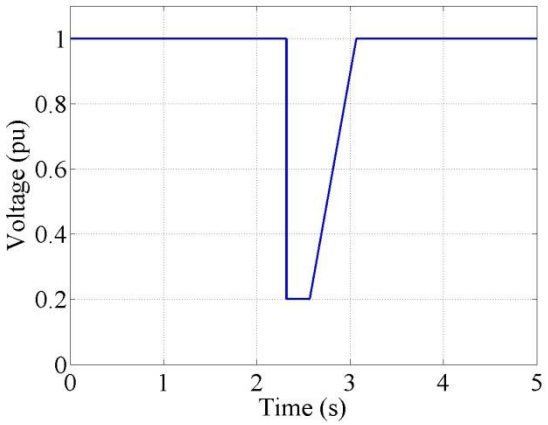

7-7: The voltage dip that the 4 kW machine is exposed to.

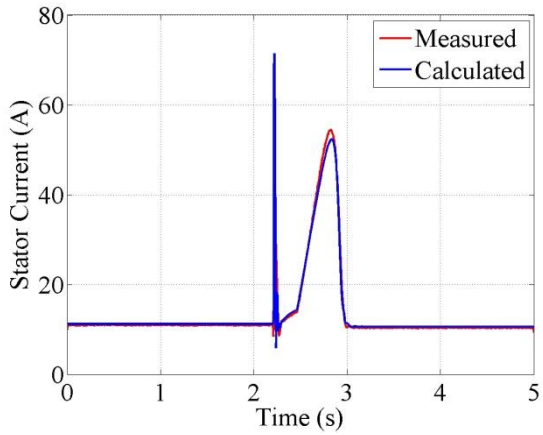

7-8: The calculated and measured stator current during the voltage dip.

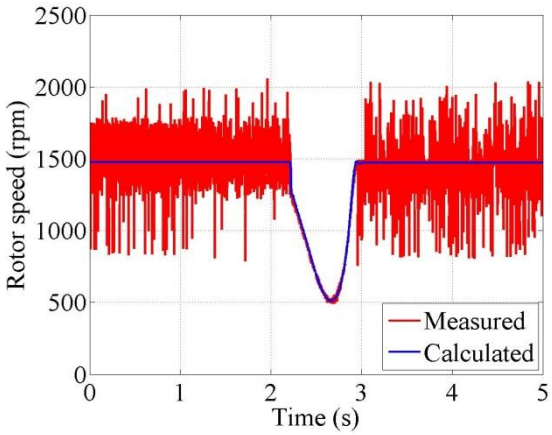

7-9: The calculated and measured speed variation during the voltage dip.

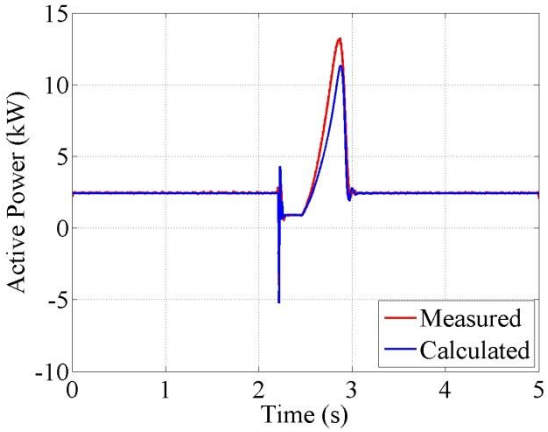

7-10: The calculated and measured active power consumed by the 4 kW machine during the voltage dip.

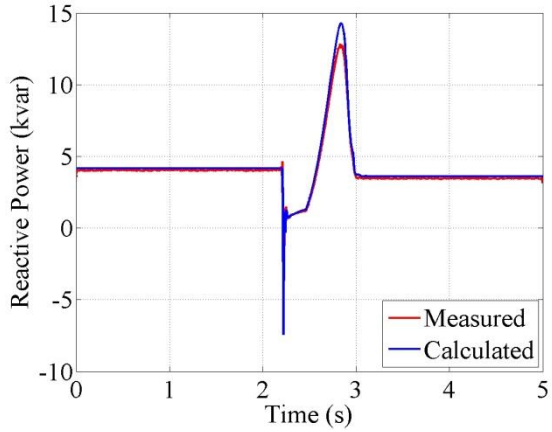

7-11: The calculated and measured reactive power consumed by the 4 kW machine during the voltage dip.

Table 7-2 includes numerical values representing the figures above at specific moments. Again the values are only valid for this specific machine.

Table 7-2: Disturbance Profile 5

Time (s)	Voltage (pu)	Speed (rpm)	Current (A)	Active power (kW)	Reactive power (kvar)
2.00	1	1476	11.02	2.47	4.08
2.21	1	1476	51.78	2.28	3.04
2.32	0.25	1075	11.90	0.87	0.95
2.45	0.25	795	13.79	0.92	1.18
2.64	0.5	510	35.93	4.87	6.03
2.82	0.75	787	54.26	12.33	12.2
2.96	0.95	1476	14.3	3.04	5.00
3.00	0.95	1469	10.62	2.47	3.60
3.20	0.95	1473	10.25	2.40	3.46

7.4 Disturbance Profile 7

In this Section simulations and measurements are compared when exposed to voltage dips according to Disturbance Profile 7. The machine is supplying a load of 65 percent, for higher loads the machine trips.

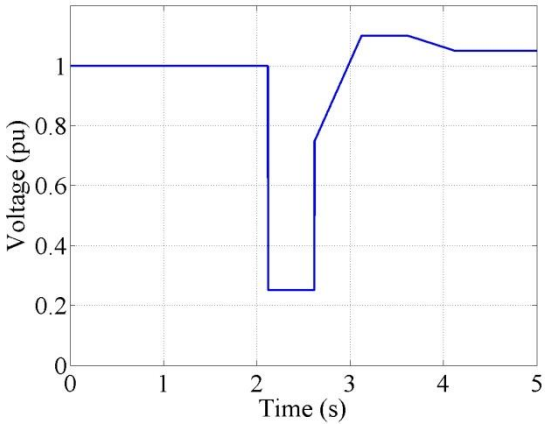

7-12: Voltage dip corresponding to Disturbance Profile 7.

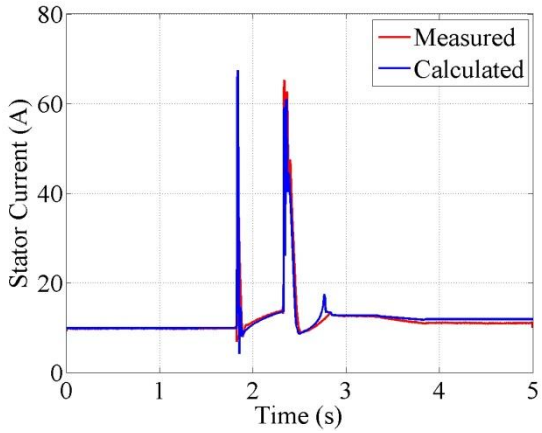

7-13: The calculated and measured stator current during the voltage dip.

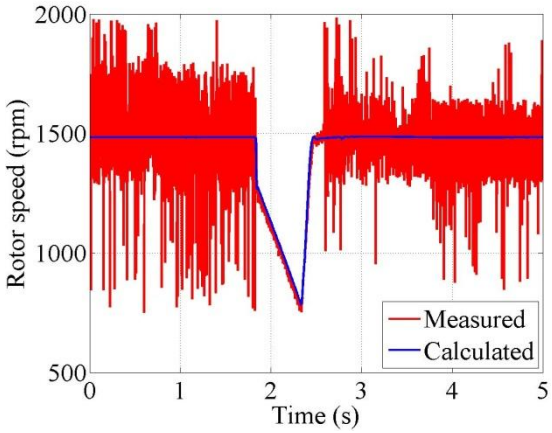

7-14: The calculated and measured speed variations during the voltage dip.

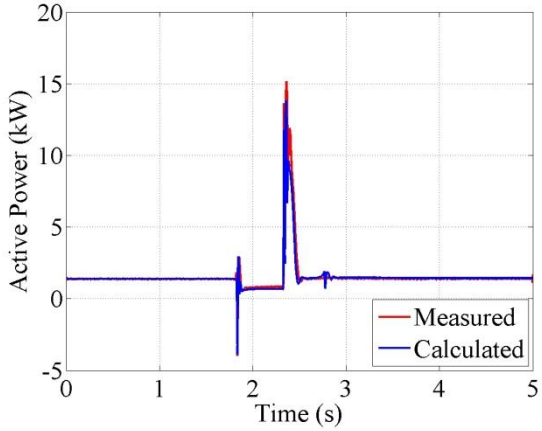

7-15: The calculated and measured active power consumed during the voltage dip.

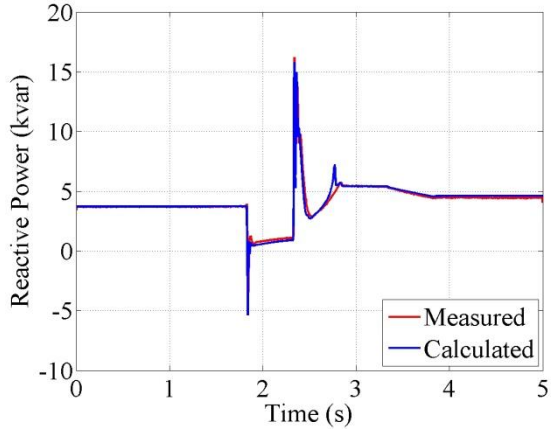

7-16: The calculated and measured reactive power consumed during the voltage dip.

Numerical values are given in Table 7-3.

Table 7-3: Disturbance Profile 7.

Time (s)	Voltage (pu)	Speed (rpm)	Current (A)	Active power (kW)	Reactive power (kvar)
1.70	1.00	1483	9.89	1.40	3.75
1.85	0.25	1275	31.44	2.89	-1.35
2.10	0.25	1028	12.24	0.83	0.93
2.33	0.25	782	65.14	1.27	1.23
2.35	0.76	844	41.59	15.2	15.21
2.60	0.94	1480	9.42	1.38	3.31
2.85	1.10	1484	12.9	1.44	5.57
3.10	1.10	1486	12.51	1.43	5.39
3.37	1.10	1486	12.36	1.45	5.30
3.60	1.07	1485	11.55	1.32	4.85
3.83	1.05	1483	10.92	1.43	4.42
4.00	1.05	1483	11.09	1.40	4.50

7.5 Disturbance Profile 12

Disturbance Profile 12 represents a voltage collapse where the voltage decreases from 1.0 to 0.7 pu during 10 minutes. Since the current will increase when the voltage decreases, the time has been shortened to twenty seconds in order to not stress the machine. This will not have any dynamical effects of the results. The frequency variation is not that important according to OKG and has therefore not been taken into account during the experiment.

The machine is loaded to a level where it consumes a current of 85 percent of rated.

The reason why the calculated and measured active power is different is unknown, but a possible reason can be the iron losses that are not considered in the simulation model.

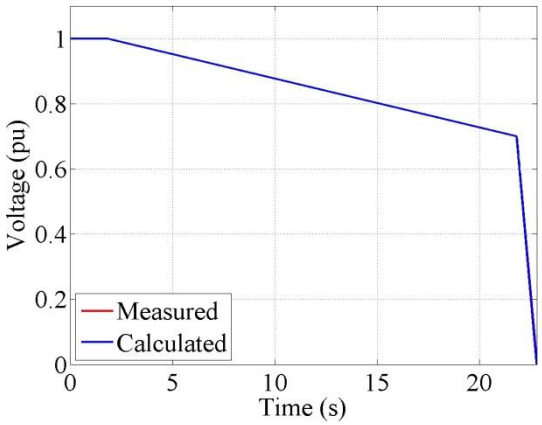

7-17: Voltage Profile 12.

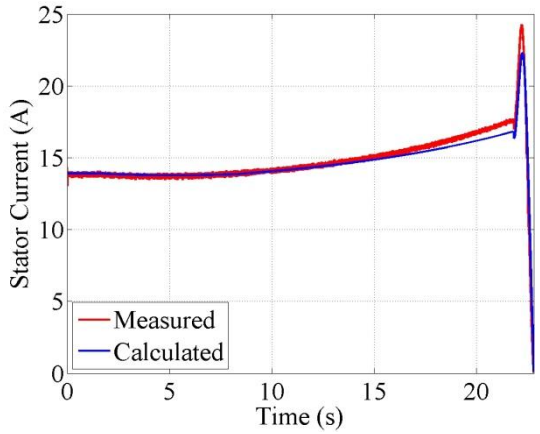

7-18: The calculated and measured stator current.

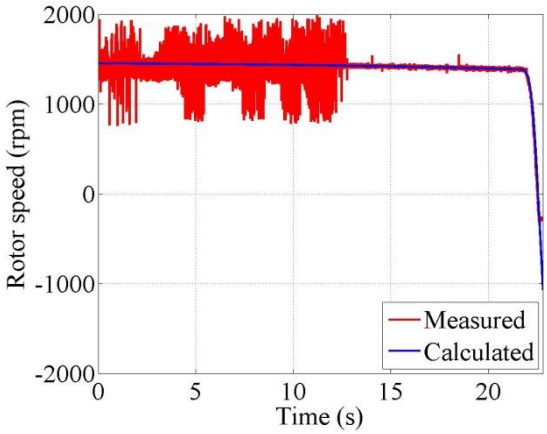

7-19: The calculated and measured speed variations.

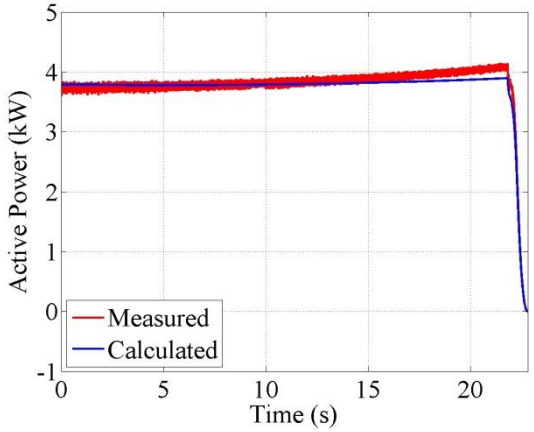

7-20: The calculated and measured active power.

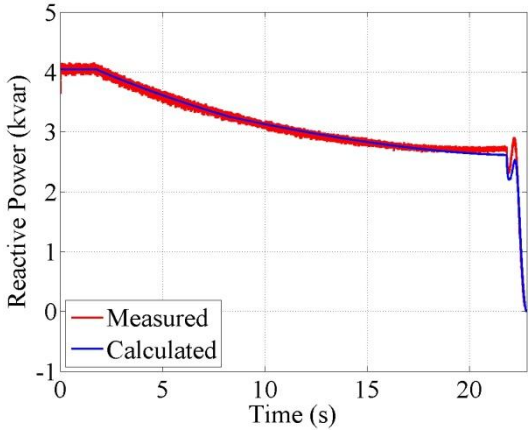

7-21: The calculated and measured reactive power.

Table 7-4 gives numerical values for some chosen moments.

Table 7-4: Disturbance Profile 12.

Time (s)	Voltage (pu)	Speed (rpm)	Current (A)	Active power (kW)	Reactive power (kvar)
1.80	1.00	1447	13.82	3.74	4.03
5.00	0.95	1442	13.71	3.76	3.58
8.00	0.91	1435	14.02	3.80	3.34
11.00	0.86	1427	14.04	3.84	3.05
14.00	0.82	1418	14.74	3.88	2.86
17.00	0.77	1405	15.79	3.97	2.79
20.00	0.73	1389	16.81	4.08	2.74
21.80	0.70	1377	17.72	4.14	2.73
22.22	0.41	1047	24.26	2.69	2.88
22.40	0.28	490	18.39	1.13	1.78
22.60	0.14	-311	8.06	0.21	0.37
22.80	0.00	-282	0.10	0.00	0.00

Before the voltage starts to fall, the machine consumes a current of 13.82 A, which corresponds to 87.5 percent. The current reaches rated current at a voltage level of 0.77 pu.

7.6 Disturbance Profile 13

As in the previous profile the frequency variation has not been taken into account during the measurements.

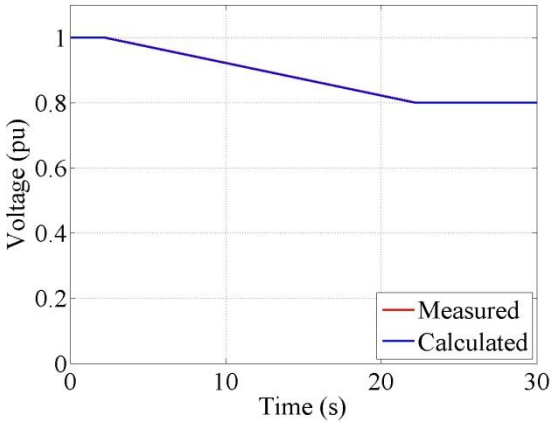

7-22: Voltage Profile 13.

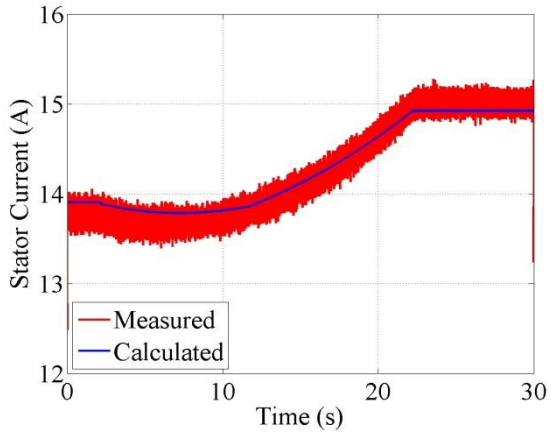

7-23: The calculated and measured stator current.

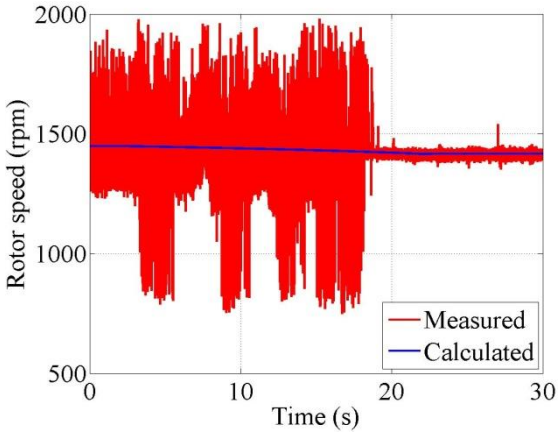

7-24: The calculated and measured speed variations.

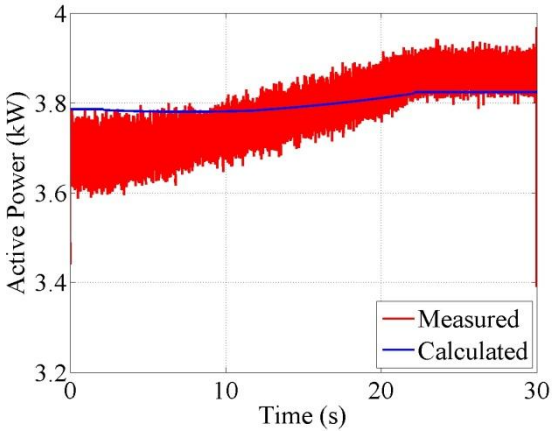

7-25: The calculated and measured active power.

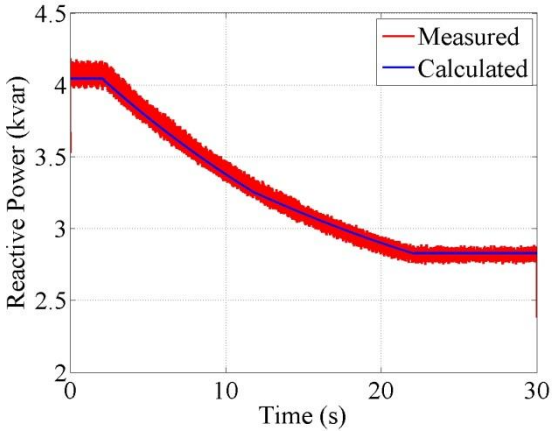

7-26: The calculated and measured reactive power.

In table 7-5 numerical values from the measurements can be seen.

Table 7-5: Disturbance Profile 13.

Time (s)	Voltage (pu)	Speed (rpm)	Current (A)	Active power (kW)	Reactive power (kvar)
2.00	1.00	1448	13.77	3.69	4.06
6.00	0.96	1444	13.70	3.72	3.70
10.00	0.92	1439	13.73	3.74	3.39
14.00	0.88	1433	14.00	3.78	3.16
18.00	0.84	1425	14.39	3.82	2.97
22.00	0.80	1416	14.98	3.86	2.83
26.00	0.80	1416	15.03	3.87	2.82

8 Conclusion

The purpose of this report was to study the behavior of asynchronous machines when exposed to irregular voltages. The main question to be answered is if the policy that not load the machines to more than 85 percent is enough to fulfill the requirements of the nuclear power industry.

When a voltage dip occurs, the speed of the motor drops and the motor is subjected to current and torque transients. During the dip, the current is increased, compared to the prefault, to provide the mechanical output power. When the voltage recovers the motor is subjected to an inrush current, first to build up the field in the airgap and then to accelerate the motor.

Since the motors investigated in this report are not heavily loaded, 85 percent, all three will probably withstand the voltage dips according to Disturbance Profile 5 and 7. After the fault, the current doesn't exceed the rated current and the inrush current during the voltage recovery is only active during some tenth of a second. It can also be seen in the trip diagram that a less loaded motor is capable of withstanding both deeper and longer dips without any risk of overheating.

When the busbar voltage is increased according to Disturbance Profile 2 due to load rejection, the magnetizing inductance becomes saturated and the magnetizing current is highly increased. As a result the stator current is increased. For the 4900 kW and 350 kW machines the current is not exceeding the rated one, but for the 90 kW machine the current increases to 129 percent of rated. There will then be a risk of overheating if the voltage is not decreased fast enough.

In Disturbance Profile 12 and 13, where the voltage is falling, the current is increasing above the rated current and there will be a risk of temperature problems. The fact that the machines are not driven at rated torque reduces these effects, otherwise the situation would be even worse.

The result from the measurements and simulations corresponds pretty well, which verifies the model used in the report. During the measurements the machine trips when it is driving a load of 85 percent of rated and is exposed to a voltage dip according to Disturbance Profile 5 and 7. It can also be seen that the speed is decreasing more during the measurements compared to the simulations. The reason is probably due to the speed-torque characteristics of the load. When using a DC machine as load, the load torque becomes constant instead of speed dependent like the torque of a pump. Probably, the machine would withstand higher degrees of load if a speed dependent load is implemented compared to the results presented in this report.

From the measurements of the 4 kW asynchronous machines it seems possible to run it down to 80 percent without quick disconnection due to high current caused by overload. Also when the voltage increases there is no high risk of quick disconnections. The current doesn't reach rated level until the voltage has increased to 112 percent. The conclusion is that the machine can operate in the region of 80 – 110 percent and will fulfill the requirements of the nuclear power industry.

The results obtained in this report agree well with earlier research.

8.1 Future work

Implement a more correct current dependent inductance to be able to perform more accurate simulations of the machine when it becomes saturated. The saturation curve at no load then has to be measured for each individual machine.

Implement iron losses to the simulation model in order to get results that agree with the measurements in a higher degree.

Using a non-controlled DC-machine as load is resulting in a constant load torque. It could be interesting to implement a rotation speed dependent load to reach the load characteristics of a pump.

9 References

Abou-Ghazala, Amr Y., El-Gammal, Mahmoud A. & El-Shennawy, Tarek I. (2009). ”Voltage Sag Effects on a Refinery with Induction Motors Loads”. Elektrika vol. 11:2, ss. 34-39.

Alstom (1999). ”MotorMaster 200, Motor protection Relays”

Analysgruppen Bakgrund (2006). ”Forsmarksincicenten den 25 juli 2006”. Nyköping: Kärnkraftssäkerhet och utbildning AB. (Bakgrund 6)

Correia de Barros, M. Teresa, Leiria, Andrea, Morched, Atef & Nunes, Pedro (2003). “Induction Motor Response to Voltage Dips”. Proceedings of the International Conference on Power Systems Transients – IPST; 2003; New Orleans. S. 1-5.

Gerardus, C. Paap, Mahadev, S. Kolluru & Owen, T. Tan (1993). ”Thyristor-Controlled voltage regulator for critical induction motor loads during voltage disturbances”. *IEEE Transactions on Energy Conversio,* Vol. 8, No. 1, pp. 100-106.

Dugan, Roger C., McGranaghan, Mark F., Beaty, H. Wayne (1996). “*Electrical Power Systems Quality”.* New York: McGraw-Hill.

Hallenius, Karl-Erik (1982). “Contributions to the theory of saturated electrical machines”, Diss, Technical Repor No. 122, Chalmers University of Technology, Gothenburg: Vasastadens bokbinderi AB.

Hallenius, Karl-Erik (1972). “Elektriska maskiner”. Lund: CWK Gleerup Bokförlag.

Hughes, Austin (2006). “Electric Motors and Drives. Fundamentals, Types and applications”. Third edition. Oxford: Elsevier.

IEEE Std 1159-2009, *IEEE Recommended Practice for monitoring electric Power Quality*, 2009.

Kovács, P.K. (1984). “Transient Phenomena in Electrical Machines”. Budapest: Elsevier.

NEA (Nuclear Energy Agency), Committee on the Safety of Nuclear Insatallations (2009). “Defence in Depth of Electrical Systems and Grid Interactions”.

Thiringer, Torbjörn (1996). “Measurements and modeling of low-frequency disturbances in induction motors”.

Appendix A. Determination of the 4 kW asynchronous machine parameters

In this appendix the parameters of the 4 kW machine, used in the experiments, are determined. This is done by making a no load and a short circuit test of the machine and the results can be seen in Table 5. The stator resistance, R_s, is measured directly on the stator windings by using a multimeter.

Table 0-1: Measured parameters of the 4 kW asynchronous machine.

Parameter	Symbol	Data values	Measured values	Unit
Rated power	P_n	4		kW
Rated voltage Y	V_n	400		V
Rated voltage Δ	V_n	230		V
Rated current Y	I_n	9.1		A
Rated current Δ	I_n	15.8		A
Rated speed	n_n	1435		rpm
Slip	s	0.0433		
Inertia	J	0.05	1.30	kgm^2
Rated torque	T_n	26.62	1.24	Nm
Stator resistance	R_s		2.51	Ω
Rotor resistance at rated operating	R_r		2.51	Ω
Stator leakage reactance	$X_{s\lambda}$		40.59	Ω
Rotor leakage reactance	$X_{r\lambda}$			Ω
Magnetizing reactance	X_m			Ω

No load test

At a no load test the motor will run close to the synchronous speed and the slip, s, becomes very small, see A.1. As a result the rotor resistance, R_r/s, becomes very large and almost no current will flow through the rotor. Therefore, the equivalent circuit for a no load test can be drawn as in Figure A-1.

$$s = \frac{n_s - n}{n_s} \tag{A.1}$$

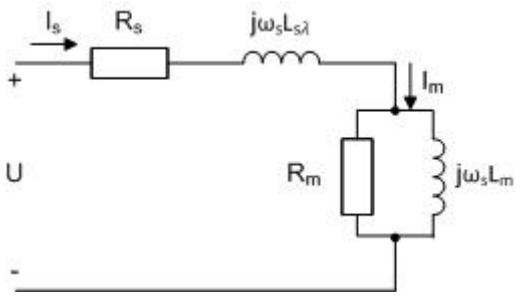

A-1: Equivalent circuit at no load test.

During the no load test the applied phase voltages and currents are measured and by making a Fast Fourier Transform, FFT, the magnitudes and phase shift is calculated. Then, by dividing the phase voltage with the current the no load impedance is calculated where the imaginary part with high accuracy can be set equal to the stator reactance (Hallenius 1972):

$$Im\{Z_{\text{no load}}\} = X_s = X_{s\lambda} + X_m \quad \text{(A.2)}$$

Short circuit test

At short circuit test the rotor is prevented from rotating and the slip becomes 1. The short circuit voltage is 12-25 percent of the rated voltage and in this case the degree of saturation is small enough to neglect the magnetizing current (Hallenius 1972).

The short circuit impedance is calculated in the same way as in the no load test and since the magnetizing current is neglected the imaginary part is set equal to the sum of the stator and rotor leakage reactances:

$$Im\{Z_{sc}\} = X_{sc} = X_{s\lambda} + X_{r\lambda} \quad \text{(A.2)}$$

The operating characteristics of the machine are sparsely affected on how X_{sc} is divided between $X_{s\lambda}$ and $X_{r\lambda}$ and in general they are set equal (Hallenius 1972):

$$X_{s\lambda} = X_{r\lambda} = \frac{X_{sc}}{2} \quad \text{(A.3)}$$

Now the magnetizing reactance can be calculated:

$$X_m = X_s - X_{s\lambda} \quad \text{(A.4)}$$

If the stator resistance is subtracted from the short circuit resistance, R_{sc}, we get a resistance, R, which is equal to the rotor resistance and rotor leakage reactance in parallel with the magnetizing reactance:

$$R = Re\{Z_{sc}\} - R_s = R_r \frac{X_m^2}{R_r^2 + (X_{r\lambda} + X_m)^2} \quad \text{(A.5)}$$

But normally $(X_{r\lambda}+X_m)^2 >> R_2^2$ and X_m is 20 – 50 times bigger than $X_{r\lambda}$, so usually the rotor resistance is set equal to the short circuit resistance minus the stator resistance (Hallenius 1972):

$$R = Re\{Z_{sc}\} - R_s = R_r \quad \text{(A6)}$$

Magnetizing Inductance

To consider saturation in calculations of the 4 kW machine, the magnetizing inductance has been determined as a function of the magnetizing current, see Figure A-2. It was done in the same way as (Thiringer 1996) by no load test performed at different voltage levels.

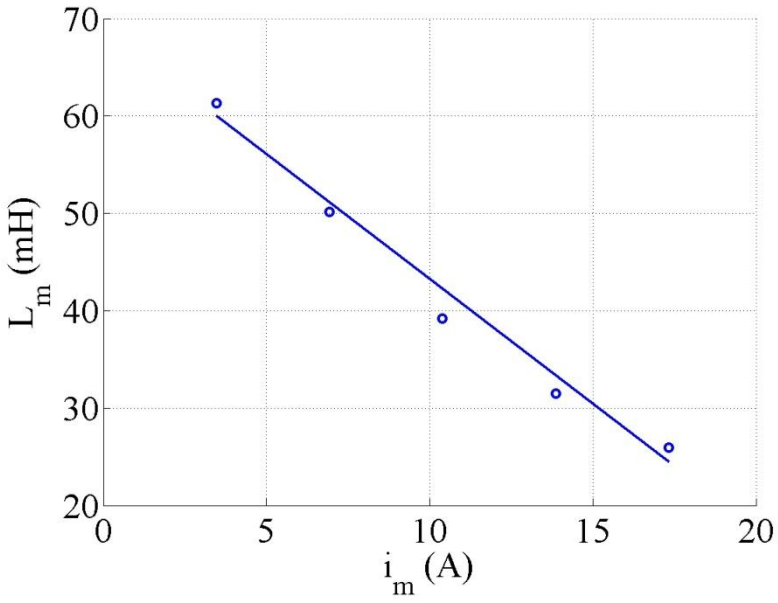

Figure A-2: Measured magnetizing inductance as a function of the magnetizing current.